



KTH Engineering Sciences

Design and Neutronic Evaluation of Thorium Fuel in Pressurized Water Reactors

LIU CHANYUN

Master of Science Thesis
Reactor Physics Department
Royal Institute of Technology

Stockholm, Sweden 2008

TRITA-FYS 2008:05
ISSN 0280-316X
ISRN KTH/FYS/--08:05--SE

© Liu Chanyun, 2008

Printed by Universitetservice US-AB, Stockholm 2008

Abstract

The purpose of this thesis is to study the feasibility of a high content thorium fuelled pressurized water reactor. The focus is on the neutronic behaviors. Thorium based fuel design options with four different fissile components are investigated. Standard uranium oxide is used as the reference fuel. The analysis is performed using the statistical codes MCNP and MCB.

First, the fuel compositions are adjusted to obtain the required discharge burnup 55 MWd/kgH.M. under a fixed power density. Next, neutron spectrum, power profile, reactivity coefficients as well as kinetic coefficients are studied.

The calculation shows a significant reduction of the quantity and quality of plutonium can be achieved if ^{233}U or MEU is used as the fissile component. Plutonium is the main source of proliferation potential and radiotoxicity generated during the irradiation of the standard UOX fuel. At the same time, although the coolant temperature coefficient for thorium with ^{233}U as fissile component is slightly positive, negative feedbacks from fuel and coolant are large enough for the safety issues during normal operation. If ^{233}U and LWR spent fuel grade plutonium is mixed properly and used as the fissile component, the breeding ratio can be about 1. The neutron spectrum created in this case is more thermal than that in case of thorium fuel with plutonium as fissile material. All the coefficients are in reasonable range. Especially, the coolant temperature coefficient is negative.

Last, a simple shutdown study was carried out. The shutdown margin is enough in both hot shutdown events and cold shutdown events.

As a conclusion, thorium fuel has similar behavior as uranium fuel in PWRs. Nevertheless, thorium fuel has more negative Doppler coefficient.

Table of Contents

Abstract	3
Table of Contents	5
Acknowledgements	7
1. Introduction.....	9
1.1. Motivation and Objectives	11
1.2. Characteristics of Thorium Fuel.....	12
1.3. History and Current State of Thorium Fuel Research.....	13
2. Methodology.....	15
2.1. Monte Carlo Calculation Method.....	15
2.2. Geometry Description of the Models.....	16
2.3. Fuel Composition	19
3. Results.....	21
3.1. Burnup Calculation	21
3.1.1. Evolution of Multiplication Factor.....	21
3.1.2. Nuclide Mass Change.....	23
3.2. Neutron Spectrum	29
3.3. Power Profiles	31
3.4. Reactivity and Kinetic Coefficients	34
3.4.1. Fuel Temperature Coefficient	35
3.4.2. Coolant Temperature Coefficient.....	36
3.4.3. Coolant Void Worth	38
3.4.4. Reactivity coefficient of Boron Concentration	40
3.4.5. Prompt and Delayed Neutrons Parameters.....	41
3.5. (Th, ²³³ U, Pu)O ₂ fuel	43
3.6. Shutdown Margin Check.....	45
4. Conclusions.....	47
Bibliography.....	49
APPENDIX.....	50

Acknowledgements

I would like to give my appreciations to

- My supervisor Janne Wallenius, for his kindness and vast patience. He has been the great source of knowledge, encouragement and guidance.
- Jan Dufek, for his enthusiastic help in both MCNP-input and computerization.
- Waclaw Gudowski, for giving me the opportunity to come to study at the Royal Institute of Technology.

I also would like to thank all other the members in the reactor physics department and friends met in Sweden. You made my life here more exciting and wonderful.

I am also grateful to my family, for their support and love.

1. Introduction

The research in nuclear field and the nuclear industry has become more and more active nowadays after more than 20 years sleeping period due to the incidents in Three Mile Island (1979) and Chernobyl (1986). Between 1970's and 1980's, a lot of countries planned to change energy to nuclear energy because nuclear energy can help them to satisfy the objective of independence, diversity and security of energy supply. The installed nuclear capacity rises from less than 1 GW in 1960 to more than 300 GW in the late 1980's. Figure 1 shows the history of the global nuclear power industry. But the two incidents mentioned above made the public scared to nuclear technology and wanted to shut down the nuclear reactors. A lot of plants planned were cancelled after these two accidents.

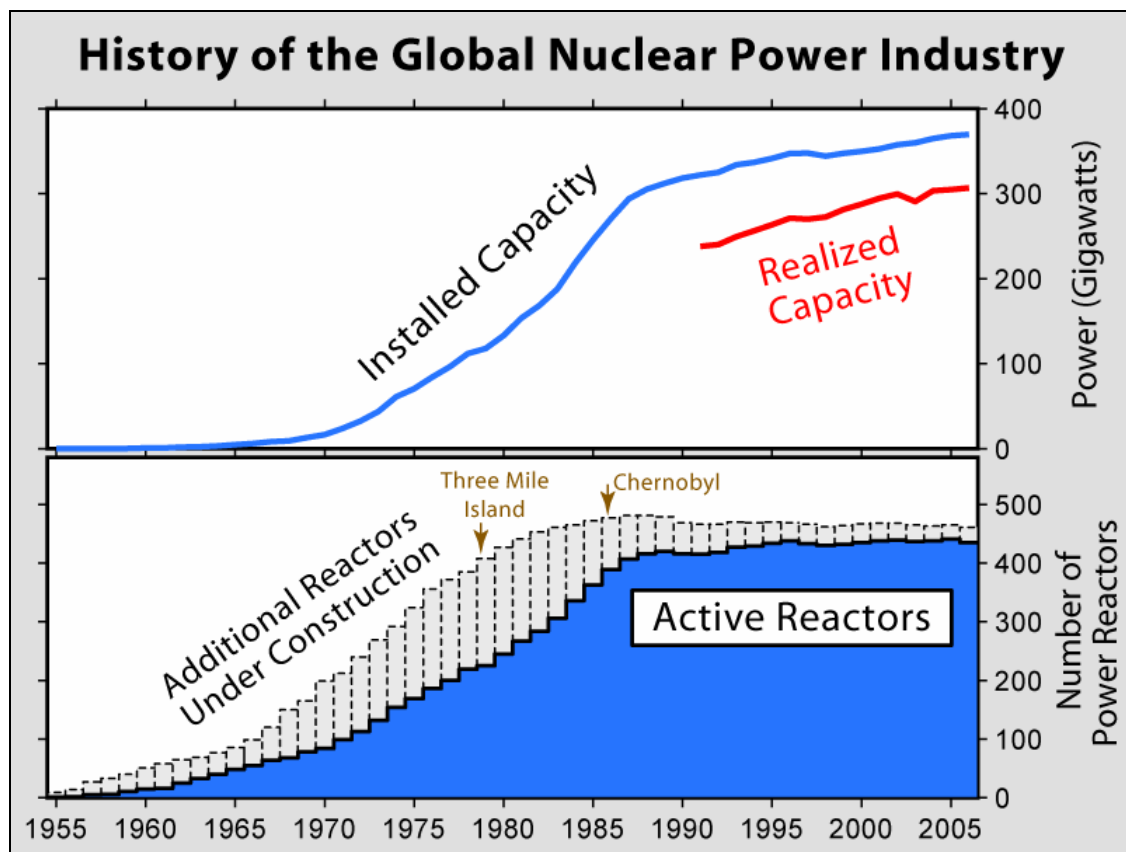


Figure 1: History of the global nuclear capacity and reactors in power industry [1]

As of August 8th, 2007, there are 439 nuclear power reactors in operation in 31 countries in the world shown in Figure 2 and tabulated in Table 1, providing 17% of the world electricity. Most of the reactors are uranium fuelled and light water

moderated. The nuclear technology performs safely, reliably and environment friendly.

Table 1: Operational Reactors by Type

Type	No. of Units	Total MW(e)
PWR	265	243233
BWR	94	84958
PHWR	44	22367
GCR	18	9034
LWGR	16	11404
FBR	2	690
Total	439	371686

PWR (Pressurized Water Reactor), BWR (Boiling Water Reactor), PHWR (Pressurized Heavy-Water Reactor), GCR (Gas Cooled Reactor), LWGR (Light-Water-cooled Graphite-moderated Reactor), FBR (Fast Breeder Reactor)

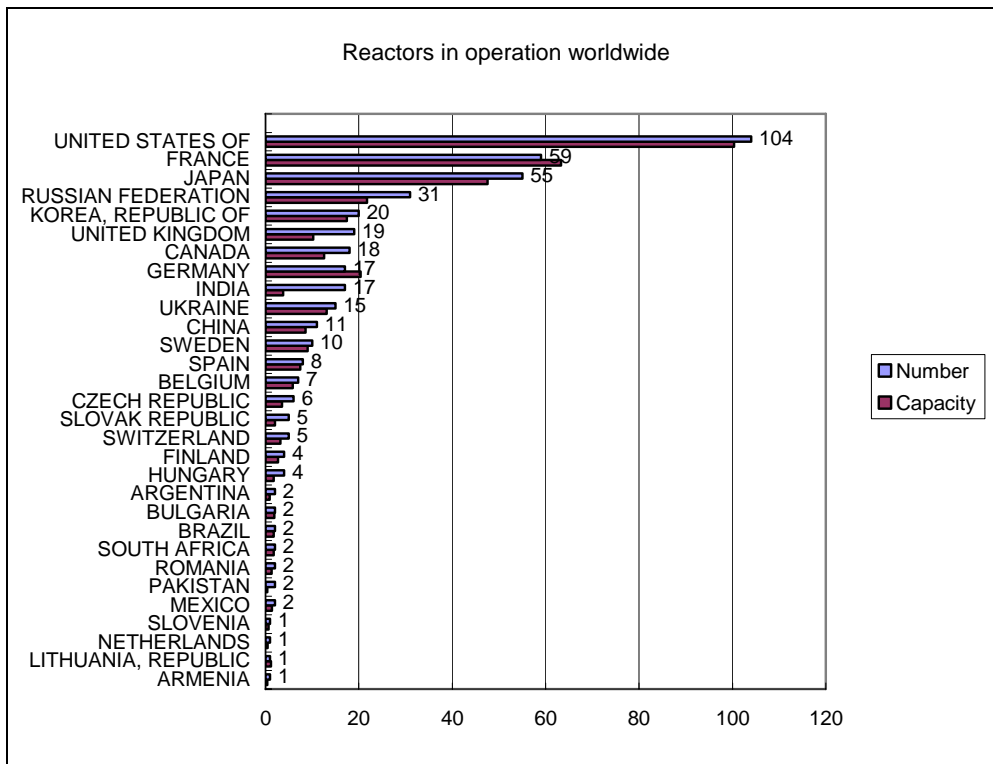


Figure 2: Number and Capacity of reactors in operation worldwide

Note1: world totally 439 reactor units including 6 reactors in Taiwan, China.

Note2: 5 long-term shutdown units are not counted.

Note3: data for capacity (in unit of GW) has been divided by a factor of 1000.

As the investigation about the two accidents and the nuclear technology develops, the public currently knows and learns more about nuclear technology than before. Other important events are the growing demand for energy as well as the concerns for environment. Unlike fossil fuel power plants, nuclear power plants do not produce greenhouse gas and it is of minimal environmental impacts. It also has competitive economics, comparing with renewable energy, such as wind power, solar power and so on. All of these aspects will provide an important role to the nuclear power. Scientists and engineers as well as the public turn their attention to the nuclear technology again. One of the most important and popular international project is the one so called Generation IV cooperating among United State, United Kingdom, Switzerland, South Korea, South Africa, Japan, France, Canada, Brazil, Argentina and European Union. The international project Generation IV is aimed to design new nuclear energy system with advanced safety, nonproliferation, highly competitive economics and minimal waste as well as natural resource utilization. Six systems were selected to develop in 2002. The investigation is currently carried out. Nevertheless, most of these designs are generally not expected to be available for commercial construction before 2030.

1.1. Motivation and Objectives

Thorium discovered by Swedish chemist Jons Jakob Berzelius in 1828 is a naturally occurring, widely distributed, easily exploitable, slightly radioactive metal. It occurs mainly as ^{232}Th isotope. The most common thorium mineral is the thorium phosphate monazite. It is about 3 to 4 times more abundant than uranium. Table 2 gives the thorium resources worldwide estimated by GeoScience, Australia in 2006. The reserve is expected to be larger than stated in Table 2. It can be about 4.5 million tons as given by IAEA-NEA 'Red book' in 2005.

In fact, some experimental power reactors based on thorium fuel were successfully operated during 1950's to 1980's. Nevertheless so far, thorium fuelled reactor hasn't been commercially used in the world which is due to some technology reasons and the sufficient uranium resources.

Nowadays, additional interest is given to thorium again, because of the proliferation resistance. The plutonium content of spent thorium fuel can be less than uranium spent fuels. Or plutonium can be burn if it is used as the initial fissile material. Furthermore, the thorium fuel cycle can improve the quality and quantity of the spent fuel. It can reduce the long-lived minor actinides production and the radiotoxicity level.

Table 2: Estimated thorium resources worldwide

Country	Tons	Percent of the world
Australia	452 000	18
USA	400 000	16
Turkey	344 000	14
India	319 000	13
Venezuela	300 000	12
Brazil	221 000	9
Norway	132 000	5
Egypt	100 000	4
Russia	75 000	3
Greenland	54 000	2
Canada	44 000	2
South Africa	18 000	1
Other countries	33 000	1
Total	2 492 000	100

The present work is to study the feasibility of high content thorium fuels in pressurized water reactors which takes up more than 60 percent of the nuclear plants in the world. The focus is on the neutronic behaviors of thorium fuel with different fissile drivers and to find a better choice.

1.2. Characteristics of Thorium Fuel

The fertile isotope ^{232}Th which is like isotope ^{238}U can absorb a neutron and become ^{233}Th . Then it decays to ^{233}Pa by β decay. Fissile isotope ^{233}U is created by β decay of ^{233}Pa . ^{233}U is a fissile isotope as ^{235}U . So, in theory, an efficient breeding cycle can be set up if some fissile material is used as the driver at the beginning.



The high thermal capture cross section of thorium will require more amount of initial fissile material as a compensatory. It will reduce the neutron capture in moderator. In addition, the neutron yield as well as fission probability of ^{233}U in thermal energy region is higher than that of ^{235}U and ^{239}Pu . Hence, thorium fuel can have higher thermal neutron utilization factor. Besides, thorium oxide has an extremely high melting point about 3300 °C.

The challenge is that, ^{233}U is always associated with ^{232}U . ^{232}U and its daughter products have strong gamma radiations which makes the process, fabrication and handling of fuel containing ^{233}U extremely difficult.

1.3. History and Current State of Thorium Fuel Research

There has been about 40 year's study on thorium fuel cycles. Nevertheless, the study is on a smaller scale compared to uranium fuel cycles or plutonium fuel cycles. It is being studied in fast reactors, light water reactors and high temperature reactors. Basic research and development has been conducted in the USA, Germany, India, Russia, Japan and the UK. Several test reactors have been partially or completely loaded with thorium fuel.

The project Dragon reactor in UK, cooperating among the UK, Austria, Denmark, Sweden, Norway and Switzerland has been operated for 741 full power days from 1964 to 1973. The AVR experimental pebble bed reactor based on thorium fuel in Germany was operated between 1967 and 1988. The maximum burnup was 150 MWd/kgH.M.. The operating time was over 750 weeks and around 95% of the time was using thorium fuel. Another thorium fuelled reactor is General Atomics' Peach Bottom high-temperature, graphite-moderated, helium-cooled reactor operated at 110 MW_{th} between 1967 and 1974 in the USA.

The only commercial thorium fuel based plant is the Fort St Vrain reactor in the USA. It was a high temperature, graphite-moderated, helium-cooled reactor and has been operated from 1976 to 1989.

Thorium fuelled Pressurized Water Reactors were investigated at Shippingport in the USA. The initial fissile materials are both ^{235}U and plutonium. Thorium fuelled light water breeder reactors (LWBR) were successfully tested from 1977 to 1982. The test LWBR was using ^{233}U as fissile material.

Another reactor, Kakrapar-1 in India, was the first reactor in the world to achieve power flattening across the reactor core using thorium, rather than depleted uranium. It achieved about 300 days of full power operation in 1995. The Kamini

experimental neutron-source research reactor started up in 1996 in India is Fast Breeder Test Reactor with the thermal power of about 30 kW. The initial fissile material is reprocessed ^{233}U from spent thorium oxide fuel. Kaiga-1 and 2 and Rajasthan-3 and 4 reactors in India were planned to use thorium. A thorium fuel utilization program in a large scale nuclear is being carried out in India nowadays.¹

There are currently four projects conducted by the U.S. Department of Energy. They are based on a proliferation resistance and a high burnup of thorium in light water reactors.

It is obvious that more and more interests are given to thorium nowadays. In theory, it can be good solutions for both proliferation resistance and nuclear waste management. It also can be a good way to increase the resource for nuclear technology.

¹ Reference: IAEA, “Thorium fuel cycle-Potential benefits and challenges”, Vienna, Austria, May 2005.

2. Methodology

All the calculations in this thesis were performed using MCNP and MCB. Two models have been used in these calculations: single pin model and assembly model.

2.1. Monte Carlo Calculation Method

MCNP, standing for Monte Carlo N-Particle Transport Code System, is developed at the Los Alamos National Laboratory. It is a general purpose, generalized-geometry, continuous energy, and time-dependent Monte Carlo transport code.

It solves problems by simulating particle collisions including scattering, absorption and fission. The particle can be neutrons, electrons or photons. MCNP and MCB can be used in any arbitrary geometry defined by surfaces. The energy range is from 10^{-5} eV to 20 MeV for neutron transport problems. Not only the multiplication factor, but also neutron flux, particle current and other quantities can be calculated.

The MCB code is used for burnup calculations. MCB stands for the Monte Carlo Continuous Energy Burnup code. The code calculates the neutron flux and material composition at the beginning of each time step which is defined by time point card. Then the probabilities of all particle collisions of each nuclide with continuous energy cross section are evaluated. New material densities and composition are updated after the evaluation for the calculation in the next step.

Monte Carlo method is a statistical method. It is particularly useful for complex problems that cannot be solved by deterministic method codes. The result is the average behaviors of all the particles. The results got from the calculations are with statistical errors. In order to make the error small enough, the number of neutrons per cycle and the number of the cycles should be large enough. Because the code simulates each particle, it takes a long time for each calculation.

In the present work, the cross section library JEFF3.1 has been used, with some lacking nuclides taken from other libraries in the MCBXL collection.

2.2. Geometry Description of the Models

The pin cell level calculation is performed in a fuel pin with coolant and zirconium cladding in a radial infinite lattice. The coolant and moderator are light water. The geometrical description and schematic view of the pin cell is given in Figure 3. No gas gap between fuel pellet and cladding is assumed. Reflecting boundary condition in radial direction is assumed. Table 3 describes the construction materials and moderator. No thermal expansion is assumed for construction material. Hence, the densities of construction materials of the fuel rods and control rod guide thimbles (G/T) as well as instrumentation thimble (I/T) are independent on the temperature.

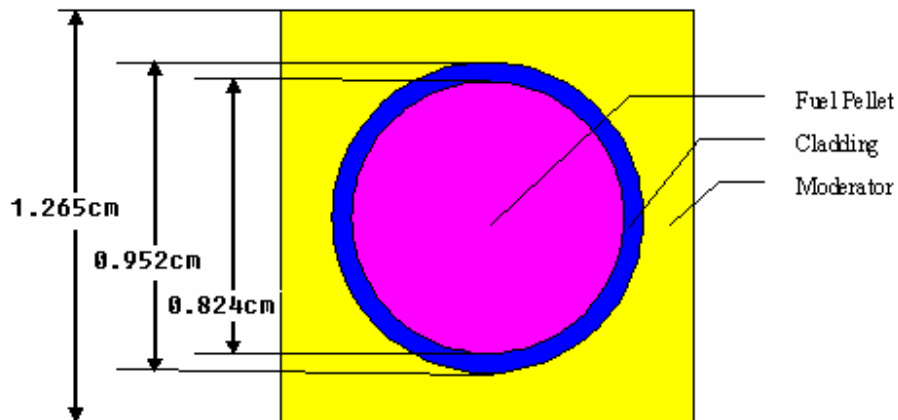


Figure 3: Schematic of cross section and parameters of the pin cell

Table 3: Density of zirconium clad and moderator

Type	Construction Material	Moderator Material
Density (g/cc)	6.5510	$6.5896 \cdot 10^{-1}$
Atomic Number Density (#/barn/cm)	$4.29826 \cdot 10^{-02}$	$6.60826 \cdot 10^{-2}$
Remarks	Structural material: cladding	
	Boron concentration: 500 ppm	

The assembly employs the standard 17x17 PWR lattice. There are 264 fuel rods, 24 control rod guide thimbles and 1 instrumentation thimble. The fuel rod structure is the same as that of in the pin cell model.

The geometrical description and schematic view is presented in Figure 4. The magenta parts in Figure 4 are fuel rods. The cream-colored parts are the control rod guide thimbles (G/T), and the cyan one is the instrumentation thimble (I/T).

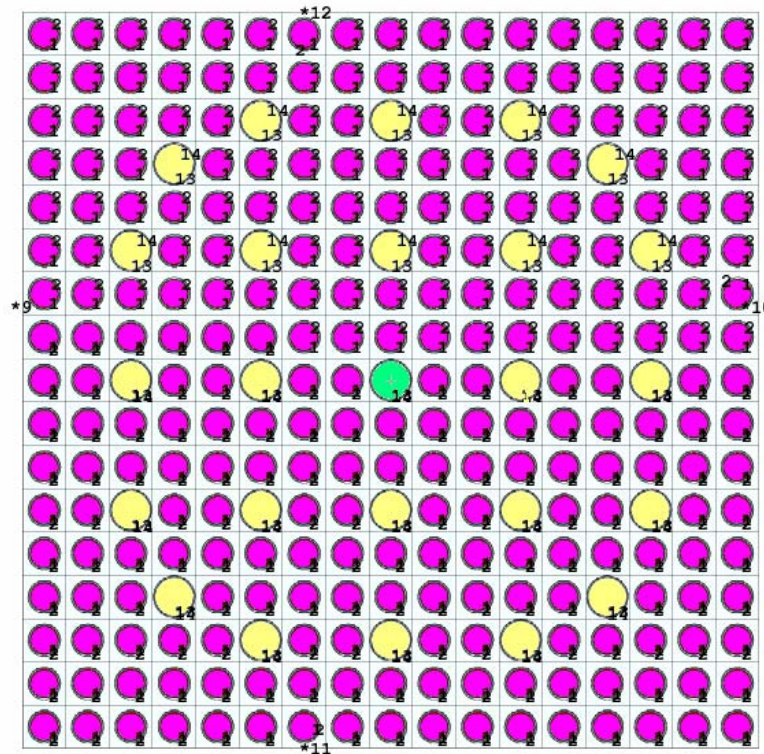


Figure 4: Radial cross section of assembly

G/T and I/T are filled with water during burnup calculations. Control rods are inserted to G/T during cold shutdown calculations. The details of the assembly are shown in Table 4.

Construction and moderator materials are the same in both pin cell and assembly models. They are tabulated in Table 3.

Isotopic composition of Zr cladding is given in Table 5. The temperature in each region is shown in Table 6.

The power density in both pin cell model and assembly model are 179 W/cm per rod. Hence, the power output is 65.5 kW in pin cell model and 17.3 MW in assembly model. 500 ppm boron is added to the coolant, corresponding to the average concentration over the cycle.

Table 4: Geometry details of the assembly²

Description	Size (cm)
Assembly pitch	21.505
Fuel rod pitch	1.265
Pellet outer diameter	0.824
Cladding inner diameter	0.824
Cladding outer diameter	0.952
G/T, I/T inner diameter	1.140
G/T, I/T outer diameter	1.220

Table 5: Atomic number densities for Zr cladding

Isotope	Atomic number density (#/barn/cm)
⁹⁰ Zr	$2.2251 \cdot 10^{-02}$
⁹¹ Zr	$4.8524 \cdot 10^{-03}$
⁹² Zr	$7.4170 \cdot 10^{-03}$
⁹⁴ Zr	$7.5156 \cdot 10^{-03}$
⁹⁶ Zr	$1.2109 \cdot 10^{-03}$

² All the geometric data for both pin cell model and assembly model are estimated from open sources

Table 6: Temperature of each region for normal operation

Region	Temperature (K)
Fuel pellet	900
Cladding	600
Moderator	600

2.3. Fuel Composition

The discharge burnup is set to be 55 MWd/kgH.M.. Three different fissile fuel components are used as the drivers in the thorium fuel. These are the reprocessed ^{233}U and LWR spent fuel grade plutonium as well as medium enriched uranium. The processed ^{233}U is 100% ^{233}U . The medium enriched uranium (MEU) is 20% enriched ^{235}U and 80% ^{238}U . Table 7 shows the LWR spent fuel grade plutonium (rgPu) composition. Thorium fuel options with these fissile fuel components are expressed as (Th, ^{233}U)O₂, (Th, MEU)O₂ and (Th, Pu)O₂. The standard uranium oxide fuel (UOX) is used as a reference fuel.

Table 7: LWR spent fuel grade Plutonium

Nuclide	Weight Percent
^{238}Pu	2.5
^{239}Pu	54.2
^{240}Pu	23.8
^{241}Pu	12.6
^{242}Pu	6.9

The initial fraction of fissile material is adjusted to obtain a multiplication factor of 1 at a burnup of 33 MWd/kgH.M. which corresponds best to the core average. The thorium fuel composition is presented in Table 8. The densities are derived by smearing dish and chamfer of fuel pellet and by assuming 95% theoretical densities.

The ^{235}U content in (Th, MEU)O₂ fuel model is higher than ^{235}U content in UOX fuel model. It is due to the higher capture cross section of ^{232}Th in thermal energy

region, which will make fewer neutrons can be absorbed by the fissile isotope. As a compensatory of this function, the amount of fissile material should be increased.

Table 8: Initial Fuel Composition

Fuel Type	Density (g/cc)	Nuclide	Weight Percent in Pin Cell Model	Weight Percent in Assembly Model
(Th, ²³³ U)O ₂	9.15	²³³ U	3.54	3.66
		²³² Th	96.46	96.34
(Th, Pu)O ₂	9.24	rgPu	8.99	8.56
		²³² Th	91.01	91.44
(Th, MEU)O ₂	9.35	MEU	26.80	25.93
		²³² Th	73.20	74.07
UOX	10.0	²³⁵ U	4.40	4.25
		²³⁸ U	95.60	95.75

3. Results

In the result part, the main results of the thesis are presented. The burnup result shows the nuclide mass change and the composition of spent fuel. Neutron spectrum and power profile are also presented. The important parameters for safety including fuel temperature coefficient, coolant temperature coefficient and delayed neutron fraction are also calculated. Finally, a simple shutdown event is simulated to check the sufficiency of the shutdown margin.

3.1. Burnup Calculation

Plutonium fuel undergoes 2 years of nature decay before it is irradiated in the core. The effective fuel power days (EFPD) are calculated to satisfy the discharge burnup of 55 MWd/kgH.M. under the fixed power density 179 W/cm per fuel rod. Multiplication factor is calculated in MCB. At the same time, neutron spectrum and power profile are also estimated. The spent fuel composition can be found in the output file.

3.1.1. Evolution of Multiplication Factor

The evolution of multiplication factor (K_{∞}) for three thorium fuels and reference UOX fuel is shown in Figure 5.³

K_{∞} for the fresh fuel varies from 1.1 to 1.4. K_{∞} of (Th, ^{233}U)O₂ fuel is the largest while K_{∞} of (Th, Pu)O₂ fuel is the smallest. This is because ^{233}U fission easier than ^{235}U and ^{239}Pu . The fission probability presented in Figure 6 is the ratio of the fission cross section to the total cross section. The thermal fission probability for ^{233}U is about 0.92, while it is for ^{235}U is 0.84 and 0.76 for ^{239}Pu , 0.70 for ^{241}Pu .

³ Solid line is for assembly model and dashed is for pin cell model in most of the figures in the results part.

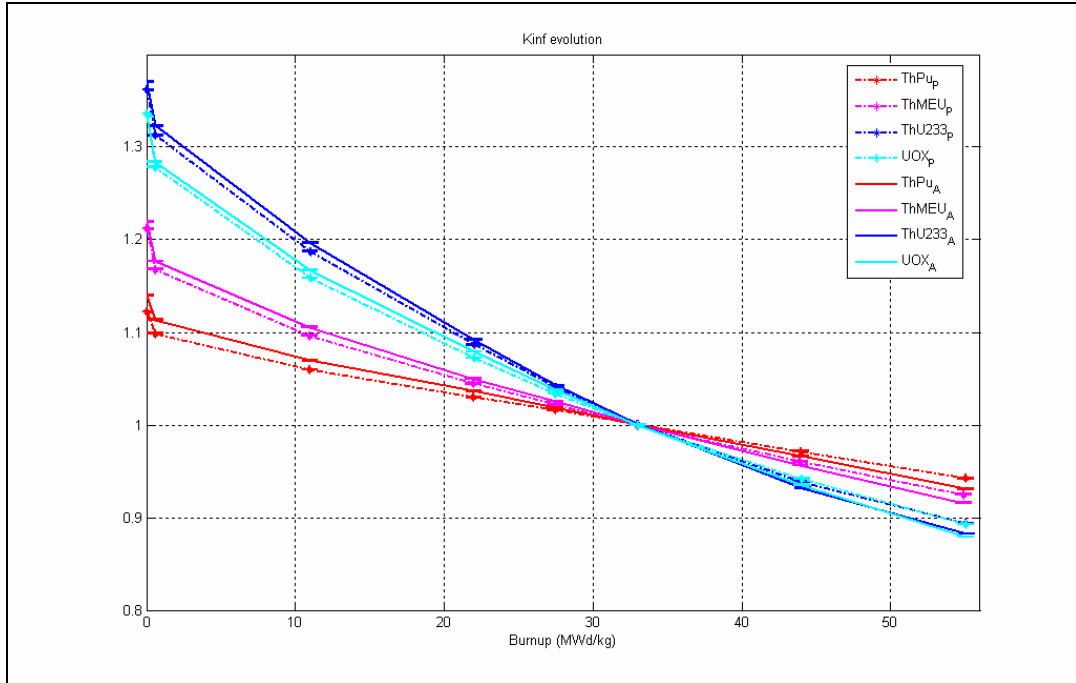


Figure 5 Multiplication factor K_{∞} as a function of burnup

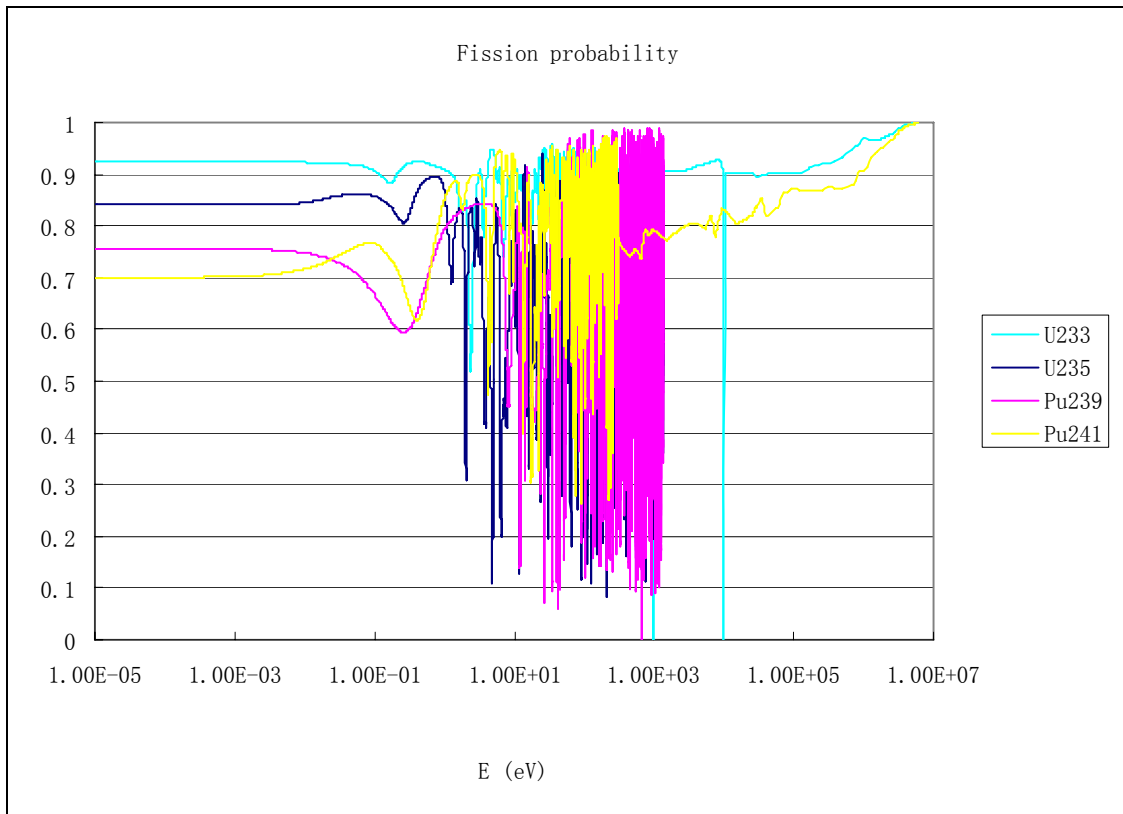


Figure 6: Fission probability

K_{∞} for all the fuels decreases with time due to the depletion of the fissile isotopes and the production of the fission products and poisons. The sharp decrease at the beginning is due to the release of ^{135}Xe . ^{135}Xe has a big neutron capture cross section and it has impact on the thermal utilization factor and thus multiplication factor. It is an important poison in reactor operation.

K_{∞} decreases to 1 at burnup of 33 MWd/kgH.M.. The decrease of K_{∞} for (Th, Pu) O_2 fuel model is the smallest. From the evolutions of K_{∞} , we see that (Th, ^{233}U) O_2 fuel can have the same K_{∞} as UOX fuel if the enrichment of ^{233}U is decreased. If K_{∞} for (Th, Pu) O_2 fuel, UOX fuel and (Th, ^{233}U) O_2 fuel are the same at the beginning, the average K_{∞} of (Th, Pu) O_2 should be the largest during the irradiation.

3.1.2. Nuclide Mass Change

Figure 7 shows the mass change of fissile isotopes as a function of burnup. And the consumption of fissile isotopes is presented in Figure 8. The fissile isotopes included in Figure 7 and Figure 8 are ^{233}U , ^{235}U , ^{239}Pu and ^{241}Pu . As mentioned before, the decrease of fissile material and the production of fission products lead to the reactivity drop. One can see from Figure 7 and Figure 8 that the amount of fissile isotopes thorium fuel consumes is smaller than the consumption of fissile isotopes of uranium fuel when they have the same burnup. The amount of fissile isotopes (Th, ^{233}U) O_2 fuel consumes is the smallest.

The change of mass of ^{233}Pa and ^{233}U is presented in Figure 9. The conversion ratio for (Th, Pu) O_2 fuel is close to that for (Th, MEU) O_2 . The amount of ^{233}U in (Th, ^{233}U) O_2 fuel drops down about 50% at the discharge burnup. The consumption of ^{233}U in (Th, ^{233}U) O_2 fuel is almost as much as the production of ^{233}U in (Th, Pu) O_2 fuel. So it is possible to use (Th, Pu) O_2 or (Th, MEU) O_2 fuelled PWRs to supply ^{233}U to (Th, ^{233}U) O_2 fuelled PWRs.

Figure 10 presents the change of mass of ^{235}U as a function of burnup. It is obvious that (Th, MEU) O_2 fuel need more uranium resource to concentrate than UOX fuel does when the same discharge burnup is required, which also can be seen from Table 8. About 78% ^{235}U is depleted in (Th, MEU) O_2 fuelled PWRs and 83% in UOX fuelled PWRs. Hence, the utilization efficiency for ^{235}U is higher for UOX fuel.

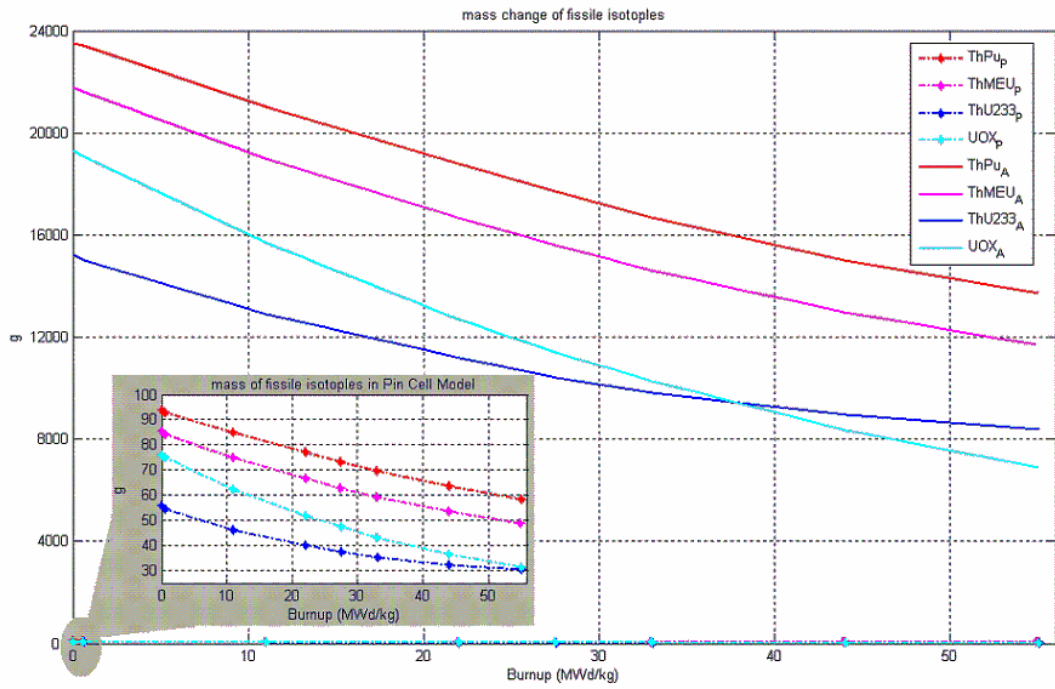


Figure 7: Mass change of fissile isotopes

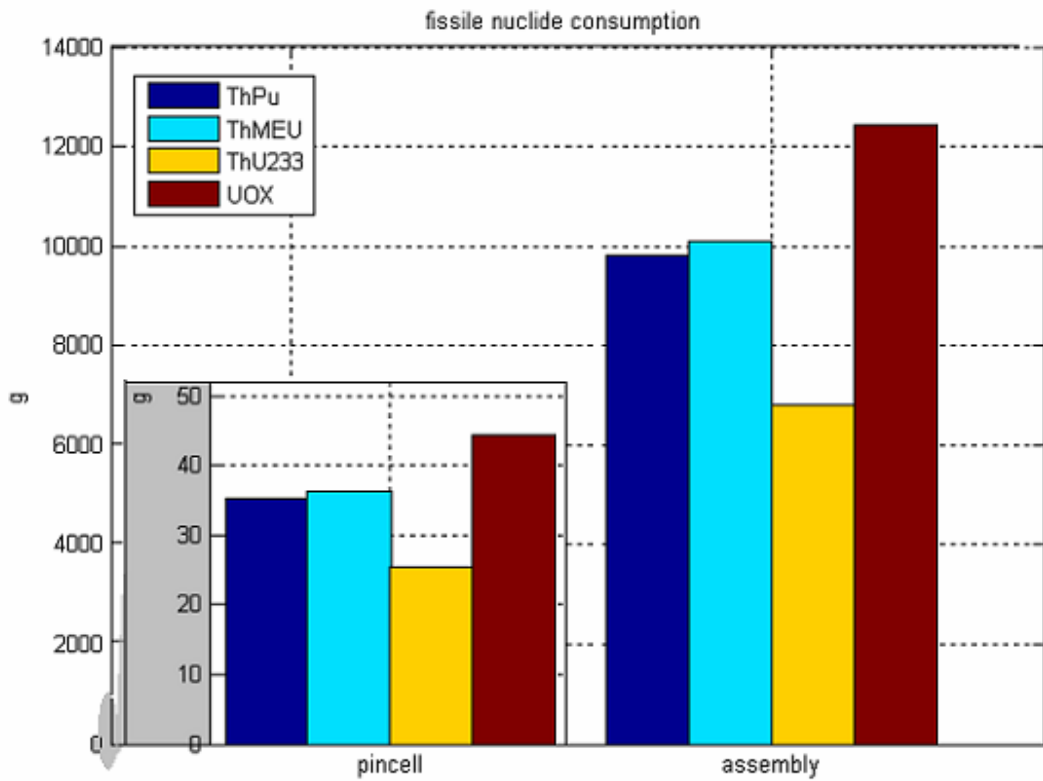


Figure 8: Fissile nuclide consumption at discharge burnup 55 MWd/kgH.M.

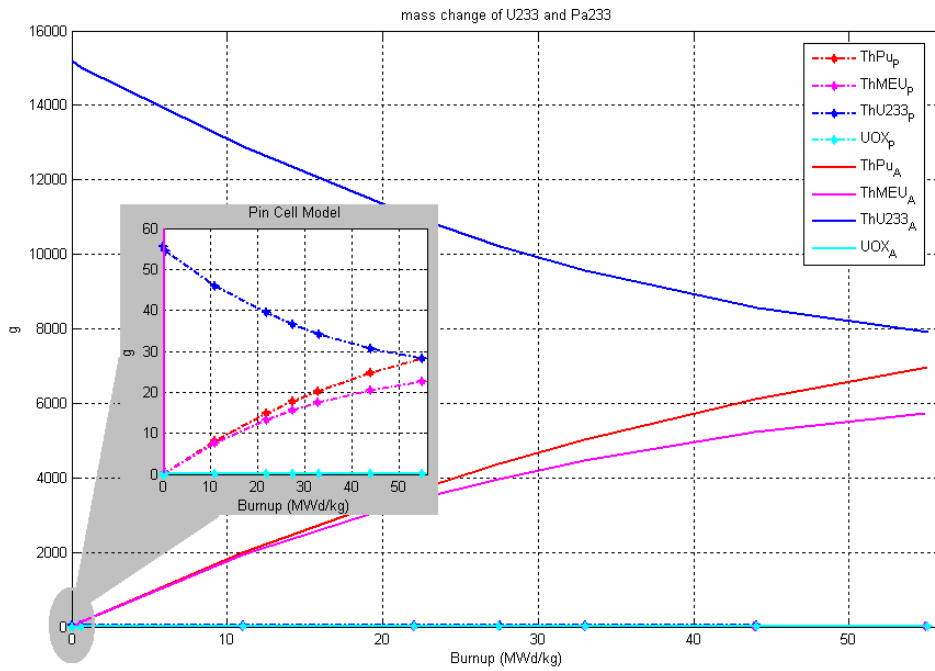


Figure 9: mass changes of ²³³U and ²³³Pa

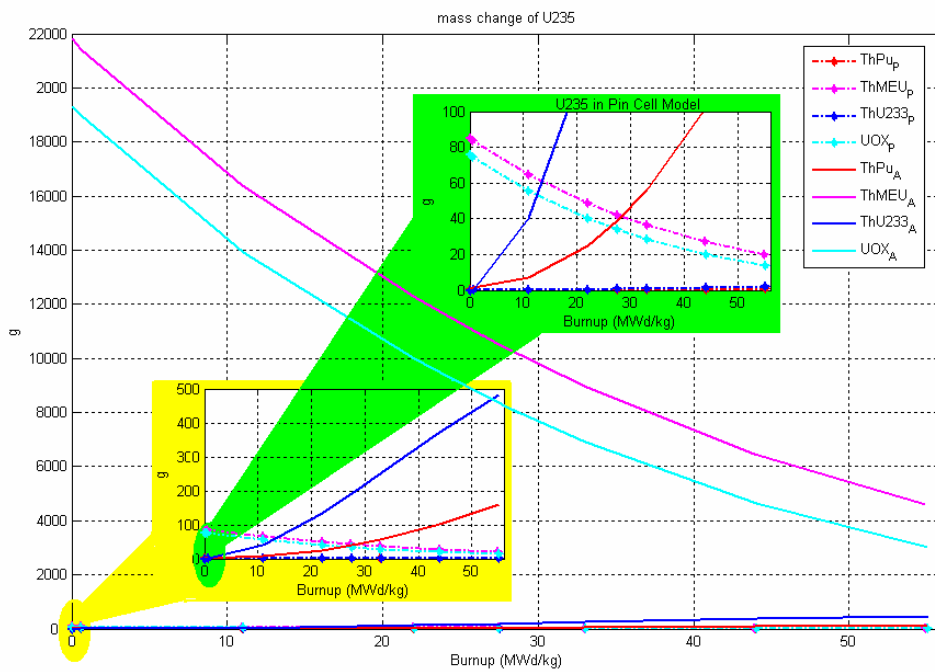


Figure 10: mass changes of ²³⁵U

^{239}Pu is formed through the capture of a neutron in ^{238}U and two consecutive β decays of ^{239}U to ^{239}Np and of ^{239}Np to ^{239}Pu . Neutron capture reactions in ^{239}Pu form ^{240}Pu . Heavier plutonium nuclides are formed from subsequent captures, and eventually higher actinides are formed through further captures and β decays. Because transuranium nuclides, whose atom numbers are higher than 92, have long half-lives and strong radiation, they are the main contributors giving the largest contribution to the radiological hazard for the first one million years in storage of nuclear waste. For example, plutonium, americium and curium have strong α - decaying. The half-lives of important actinides are shown in Table 9.

Table 9: Half-lives of important actinides, JEFF-3.1 data

Nuclide	Half life
^{238}Pu	87.7 a
^{239}Pu	24100 a
^{240}Pu	6560 a
^{241}Pu	14.3 a
^{242}Pu	$3.74 \cdot 10^5$ a
^{241}Am	433 a
$^{242\text{m}}\text{Am}$	141 a
^{243}Am	7360 a
^{242}Cm	163 d
^{243}Cm	30.0 a
^{244}Cm	18.0 a
^{245}Cm	8500 a

Table 10 displays the utilization of plutonium, americium and curium in both pin cell model and assembly model. Negative value indicates nuclide is produced. The mass changes for plutonium, americium and curium in $(\text{Th}, ^{233}\text{U})\text{O}_2$ fuel are around zero. And plutonium is the most important for nuclear weapon. $(\text{Th}, ^{233}\text{U})\text{O}_2$ fuel has the biggest proliferation resistance and it can improve the quality of the nuclear waste. The mass of plutonium in UOX increases about 1.8 times more than it does in $(\text{Th}, \text{MEU})\text{O}_2$ fuel. Accordingly, UOX model produces 1.7 times amount of Am more than $(\text{Th}, \text{MEU})\text{O}_2$ does and 2.7 times for Cm. $(\text{Th}, \text{Pu})\text{O}_2$ model can reduce around 3 times the amount of Pu created in UOX fuel model, whereas it produces around 5 times the amount of Am and 9 times the amount of Cm as the UOX model.

Table 10: Consumption of Pu, Am and Cm

Nuclide	Fuel Type	Pin Cell (g)	Assembly (g)
Pu	(Th, Pu)O ₂	74.25	19474.90
	(Th, MEU)O ₂	-8.75	-2009.30
	(Th, ²³³ U)O ₂	-0.01	-1.96
	UOX	-25.03	-5810.60
Am	(Th, Pu)O ₂	-3.47	-860.90
	(Th, MEU)O ₂	-0.24	-58.40
	(Th, ²³³ U)O ₂	0.00	0.00
	UOX	-0.65	-162.80
Cm	(Th, Pu)O ₂	-2.84	-694.38
	(Th, MEU)O ₂	-0.08	-20.34
	(Th, ²³³ U)O ₂	0.00	0.00
	UOX	-0.30	-74.36

Figure 11 and Figure 12 show the change of mass of important actinides in four fuel models. And the data in Figure 11 and Figure 12 for pin cell model has been multiplied by a factor of 264. It is obvious from Figure 11 and Figure 12 that the mass of ²³⁸Pu and ²⁴⁰Pu decrease only in (Th, Pu)O₂ fuel model and the created amount of ²⁴³Am and ²⁴⁴Cm are the largest in (Th, Pu)O₂ fuels.

Thus, it can be seen that thorium fuel can improve the quantity and quality of nuclear waste. And it also is proliferation resistant.⁴

⁴ In fact, thorium fuels are only proliferation resistant as long as they are used in a mixed neutron spectrum (like the PWR). In a well thermalized spectrum where (n,2n) reactions on ²³³U are absent, one may breed clean ²³³U without production of ²³²U.

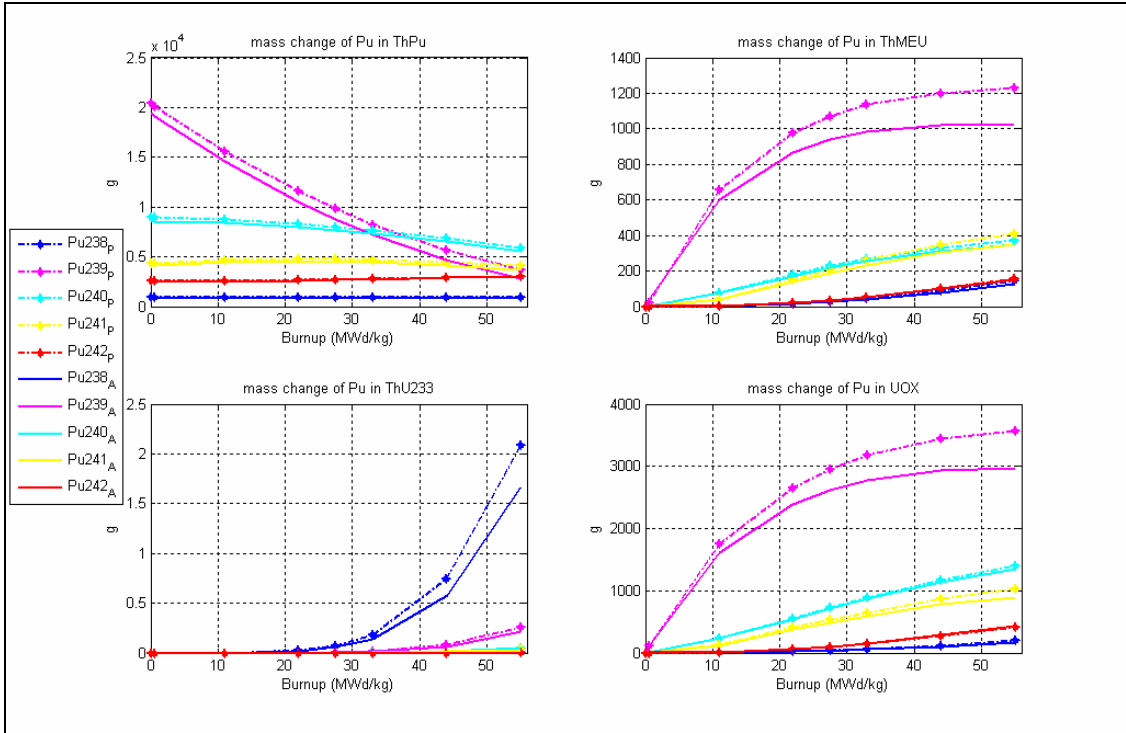


Figure 11: mass changes of Pu in four fuel models

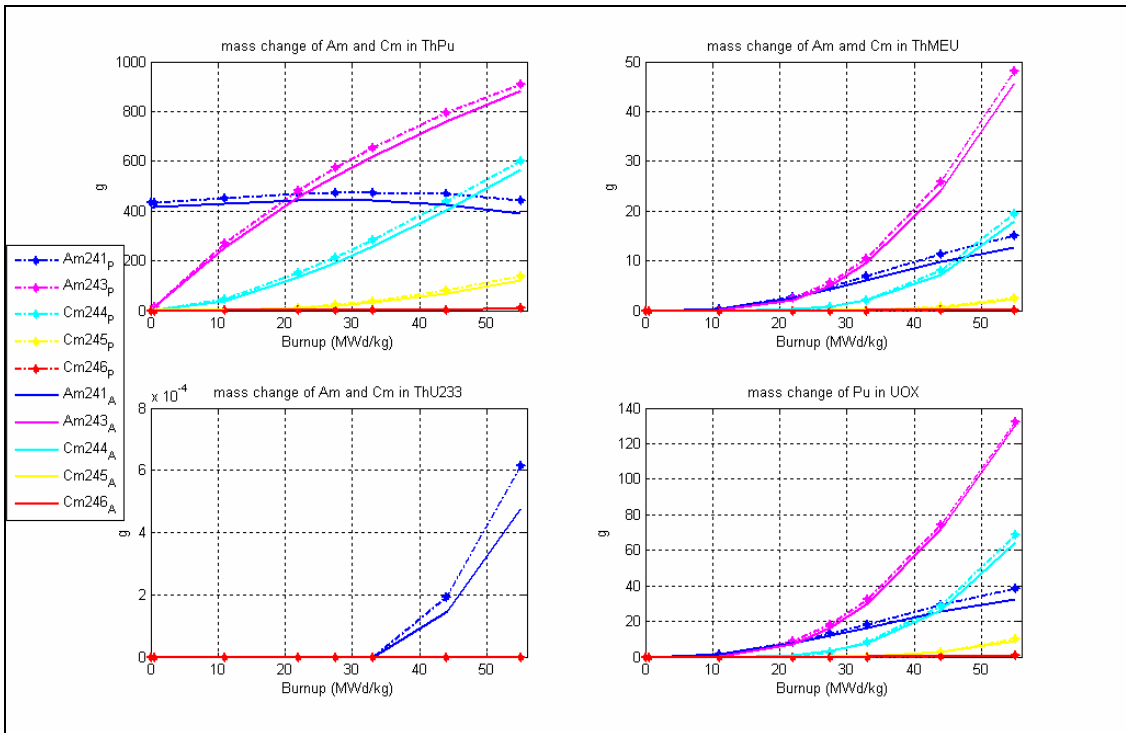


Figure 12: mass changes of Am and Cm in four fuel models

3.2. Neutron Spectrum

The neutron spectrum can be calculated by F4 tally in MCNP. The definition of F4 tally used in this thesis to get the spectrum is presented in Equation (2). Figure 13 and Figure 14 show the neutron spectrum in the fuel got from assembly calculation.

$$F4 = \sum_{n=1}^{SN} \rho_n \quad (2)$$

Where SN is the total number of simulated neutrons and ρ_n is the total length of trajectory of n_{th} neutron simulated in volume V .

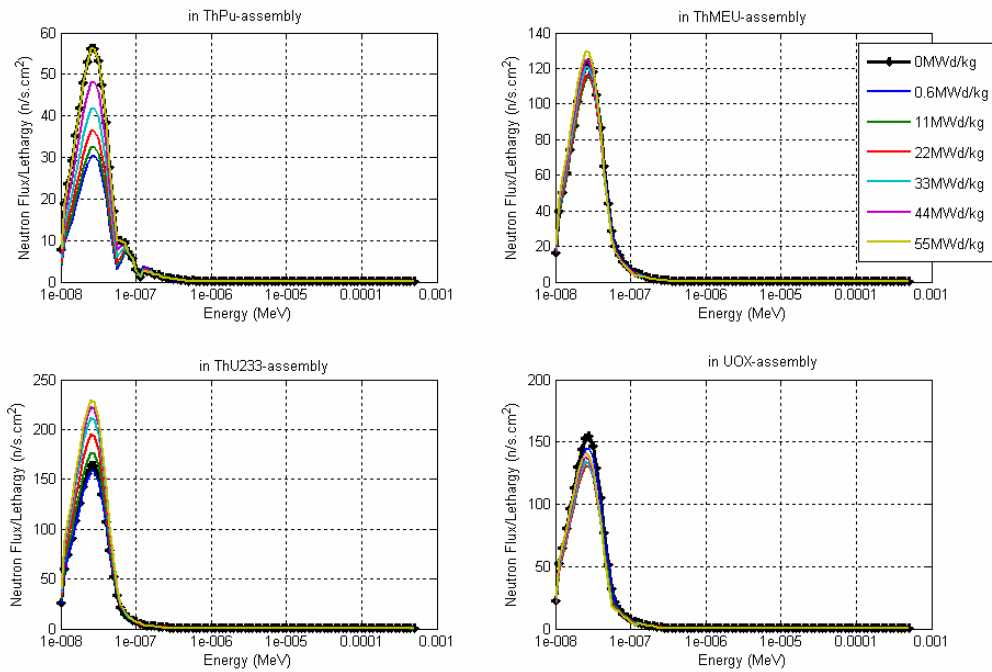


Figure 13: Neutron spectrum in the fuel average over the assembly.

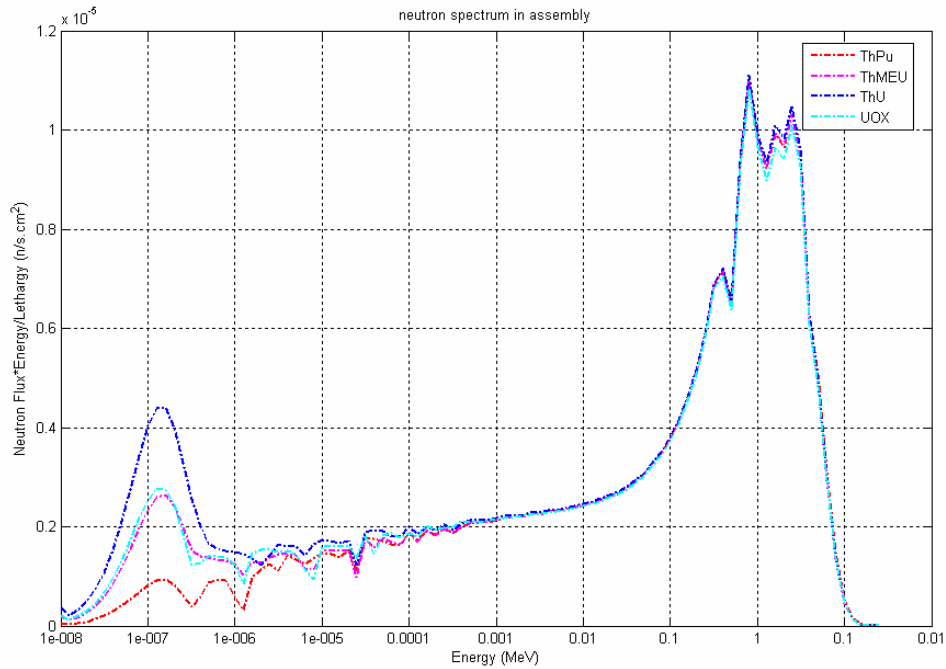


Figure 14: Flux weighted neutron energy spectrum average over the assembly in the four fuel models at burnup of 33 MWd/kgH.M..

As the fuel compositions are changing, the spectrum shifts a little versus burnup. It stands to reason, that uranium fuelled model breeds a more thermal spectrum than the plutonium fuelled model does. It is because plutonium fuel has higher total microscopic cross sections and the fissile isotopes of plutonium have some wide resonances in the epithermal energy region. (Th, ^{233}U) O_2 fuelled model generates the most thermal spectrum than (Th, MEU) O_2 fuelled model and UOX fuelled model do. The reason is similar that the total microscopic cross section of thorium is higher than uranium. The higher total cross section and the wider resonance result in a stronger spectrum depression. It is clearly visible, that there are two dips between 0.1 and 1.1 eV in spectrum of (Th, Pu) O_2 model, which correspond to the high cross sections peaks at those energy regions of ^{238}Pu and ^{240}Pu , respectively. The cross section is displayed in Figure 15 and Figure 16.

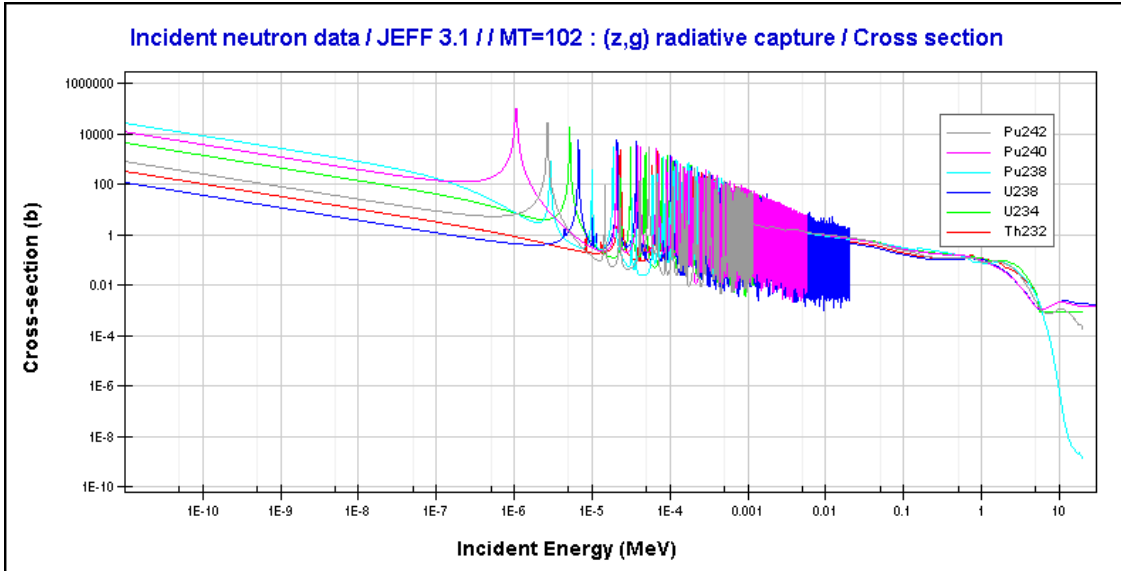


Figure 15: Microscopic Capture Cross Section of fertile isotopes

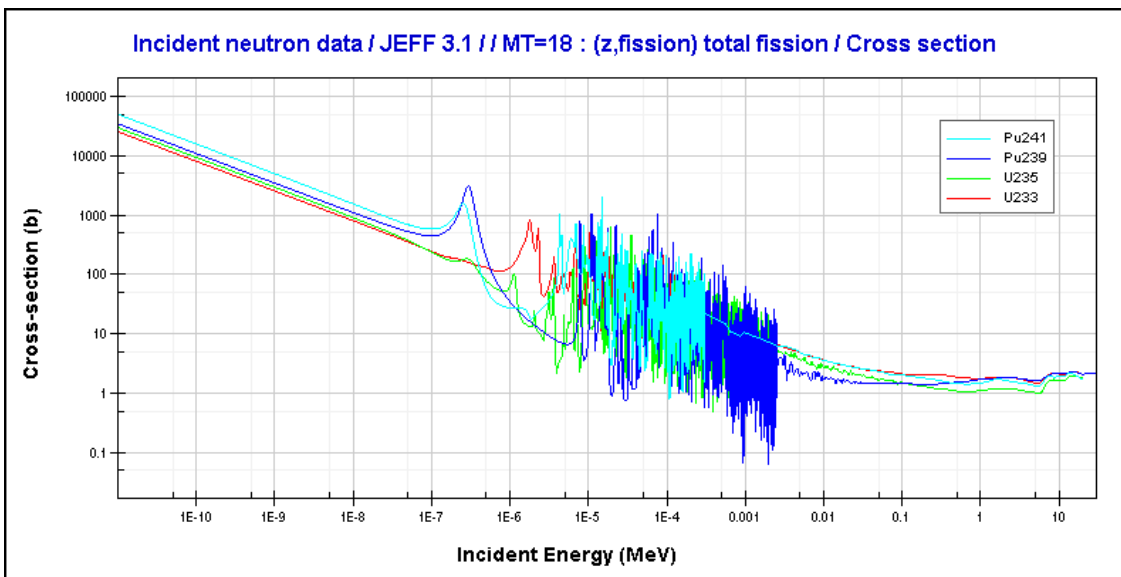


Figure 16: Microscopic fissile Cross Section of fissile isotopes

3.3. Power Profiles

The F6 tally in MCNP is used to estimate the average energy deposition over a cell. The cross section of the assembly is symmetrical in respect to origin. Hence, the radial power distribution is also symmetrical in respect to origin. The power distribution in the selected positions, which are shown as the red rods on the left

side of Figure 17, is used to express the radial power distribution.⁵ The right side of Figure 17 is the vertical cross section of the assembly. 24 surfaces are used to divide the assembly into 26 vertical cells. The energy deposition in each vertical cell is calculated. And the axial power distribution is expressed using the energy distribution in vertical cells.

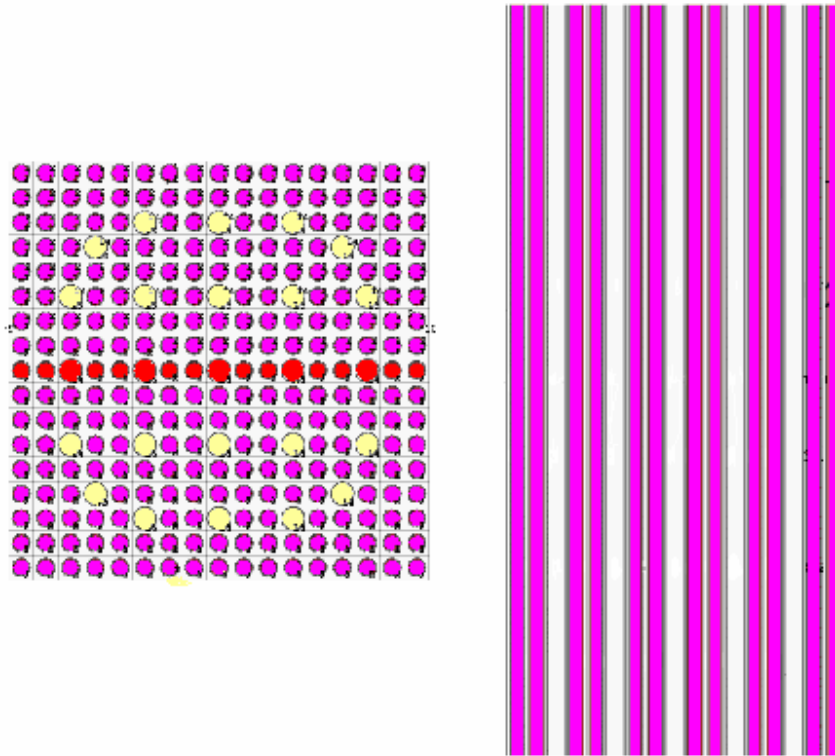


Figure 17: Assembly with radial and axial section

The power distributions are important for thermal hydraulic analysis and safety analysis. One of the parameters are the power peaking factors presented in Equation(3), (4) and(5). It is the highest local power density to average power density. The positions of the control rod and fuel optimization are also designed based on the peaking factors. The power peaking factors shouldn't be too large in order to prevent fuel rod melting. The detailed three dimensional core power distributions are monitored in operating reactors.

Figure 18 and Figure 19 display the radial power profile and axial power profile in assembly at burnup 33 MWd/kgH.M., respectively. Since the statistical error is

⁵ The result is only an indication. But this analysis is not complete. Because there is one bundle symmetry and that is octant. The power in all pins belonging to one octant should be calculated to correctly determine the radial peaking factor. The analysis here does not catch the possibility that the maximum pin power occurs at a pin outside this line. Due to the time limit, a complete analysis is not performed.

very large, the shape of the profile doesn't look so regular. But they are sufficient to figure the power profile in assembly. Several spikes appear because of the empty thimbles. There is no power output there. It is assumed the factors around the empty thimbles equates to the value nearby in Figure 18 and Figure 19. The empty thimbles make the power distribution more evenly.

$$F_r = \frac{P_{\max}^r}{P_{\text{ave}}^r} \quad (3)$$

$$F_a = \frac{P_{\max}^a}{P_{\text{ave}}^a} \quad (4)$$

$$F_t = F_r \times F_a \quad (5)$$

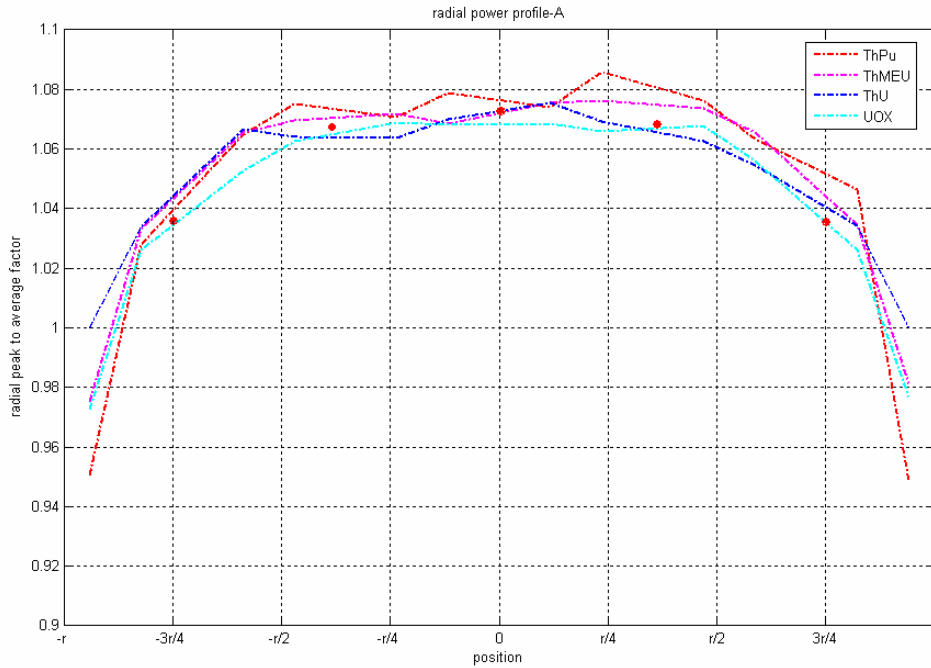


Figure 18: radial power peak to average factor

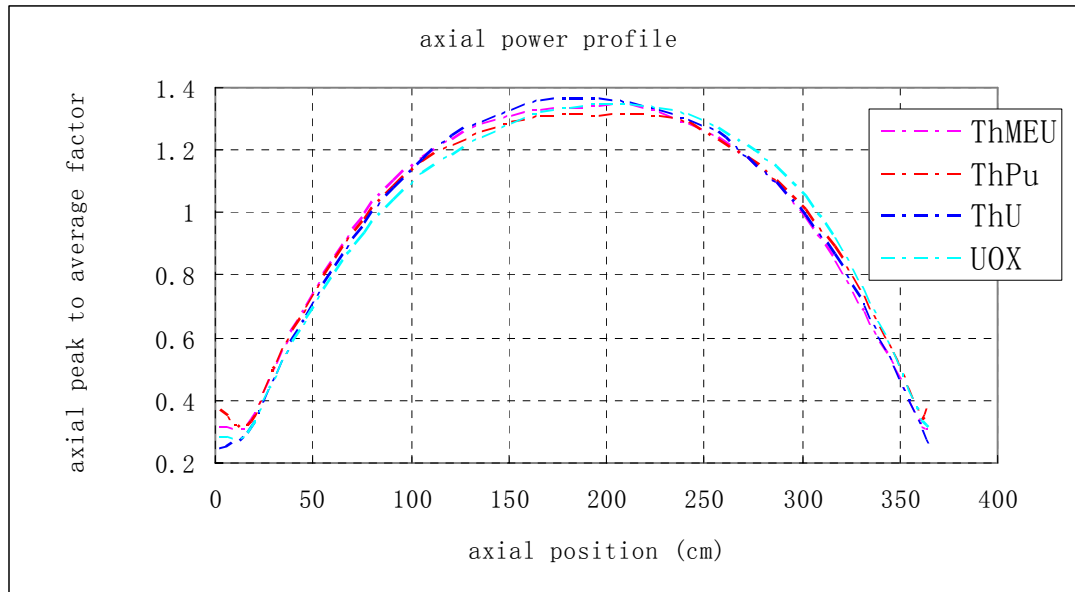


Figure 19: axial power peak to average factor

The minimum factor in radial direction occurs at the boundary of the assembly due to leakage. But the minimum axial factor isn't at the bottom or at the top of the assembly, especially for (Th, Pu)O₂ fuel. It is because of the reflector above the top of the assembly and that under the bottom of the assembly. The maximum power peaking occurs at the middle of the assembly. The axial peaking factors are around 1.40. In order to fulfill the safety limits, control rods or burnable poison can be added to the reactor to modify the power profile.

The place of the peaking factor will lead to an enhanced thermal stress and the local fuel depletion is higher. Hence, the local power profile will cause the local fuel inventory change. Then the difference will change the power profile. Hence, the power profile is shifting during fuel is burn. The most even power profile will usually be achieved at the discharge burnup.⁶

It can be seen from Figure 18 and Figure 19 that, uranium fuel has a smoother radial power profile while it also has a larger axial power peaking factor than plutonium fuel. (Th, ²³³U)O₂ has the largest axial power peaking factor.

3.4. Reactivity and Kinetic Coefficients

⁶ Due to the way to describe the material in calculation, this effect on the power profile hasn't been studied in this thesis.

Reactivity coefficients and kinetic coefficients are important safety parameters. Fuel Doppler coefficient, moderator coefficient, reactivity coefficient of boron concentration and delayed neutron parameters are calculated in this thesis. Negative coefficients bring negative feedback which is of importance for reactor operation. Generally, negative fuel coefficient and coolant coefficient are required.

3.4.1. Fuel Temperature Coefficient

Temperature coefficients include fuel Doppler coefficient and moderator temperature coefficient.

Fuel Doppler coefficient is the fuel temperature coefficient of reactivity (FTR), and can be calculated according to Equation(6)

$$FTR = \frac{\rho^{T_2} - \rho^{T_1}}{T_2 - T_1} \quad (6)$$

Where the reactivity ρ is can be expressed as Equation(7)

$$\rho = \frac{k_{eff} - 1}{k_{eff}} = 1 - \frac{1}{k_{eff}} \quad (7)$$

FTR is also called prompt reactivity coefficient. It is an inherent, prompt, negative feedback. Some isotopes have large resonances in the neutron capture cross sections in the epithermal energy region. When the temperature increases, the thermal movement of heavy nuclei becomes more vehement. The Doppler Effect between the moving nuclei and the incoming neutron will make the resonance peaks in capture cross section broadened. The probability of neutron capture increases which will decrease the reactivity. In the epithermal energy region, the microscopic fission cross-section will increase in the same way as for capture cross section if the material temperature increases, Nevertheless, for fertile nuclides the absolute increase in capture cross section is much larger than the absolute increase in fission cross section, which will grow on the reduction of reactivity. So, Doppler coefficient is dependant on the fuel composition.

In order to calculate the Doppler coefficient, multiplication factors are calculated at fuel temperature of 900 K and 1200 K respectively. Coolant temperature and cladding temperature are 600 K. Figure 20 displays FTR as a function of temperature. The unit is pcm/K.

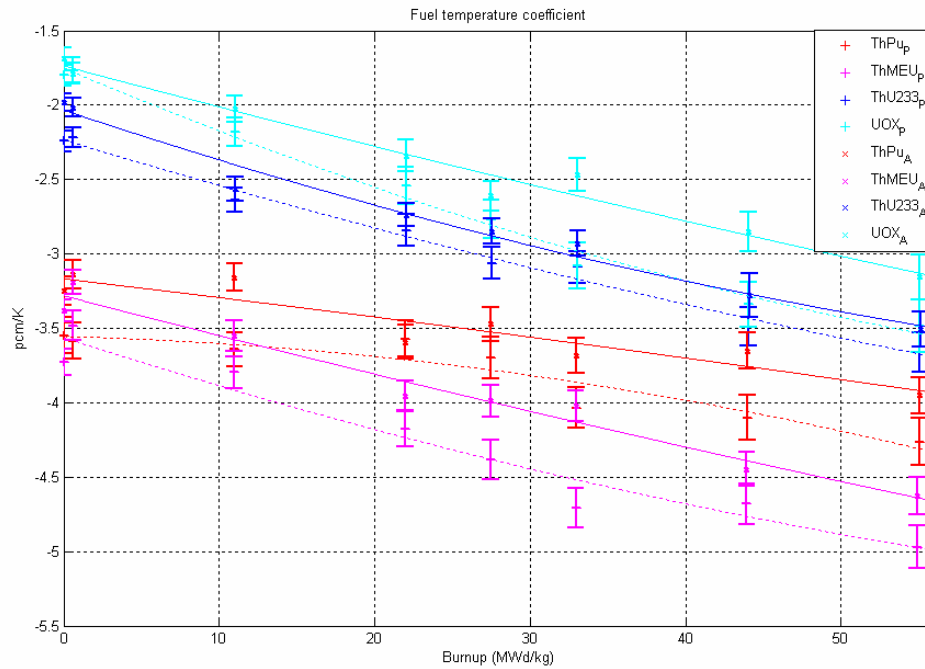


Figure 20: Fuel temperature coefficient with statistical error versus burnup

All the Doppler coefficients are negative. They are in the expected range. It is clearly visible that, thorium fuel has more negative Doppler coefficient than uranium fuel has. The reason is that, resonance broadening is more effective in ^{232}Th than in ^{238}U , which gives the more negative Doppler coefficient. $(\text{Th}, \text{Pu})\text{O}_2$ has larger negative Doppler coefficient than $(\text{Th}, ^{233}\text{U})\text{O}_2$ has. Nevertheless, $(\text{Th}, \text{MEU})\text{O}_2$ has the largest negative Doppler coefficient while UOX has the least negative values.

3.4.2. Coolant Temperature Coefficient

Moderation temperature coefficient (MTC) is an important parameter for fuel and core design in terms of light water reactor safety criteria. It is delayed temperature coefficient comparing with FTR. It can be calculated analogically to the FTR, according to Equation(6) and(7).

The coolant flowing through the reactor is at a temperature of roughly 315 °C, the pressure in the primary coolant loop is usually around 15 MPa at which the saturated temperature is 342 °C. MTC is calculated by using the perturbation card of MCNP. Multiplication factor is calculated when fuel temperature is 900 K and coolant temperature is 600 K. 20 K decrease of coolant temperature is introduced

by using perturbation card. In fact, the perturbation card changes the coolant density at 600 K, 15 MPa to coolant density at 580 K, 15 MPa. The change of the multiplication factor is calculated automatically. Figure 21 displays MTC as a function of burnup. The unit is pcm/K.

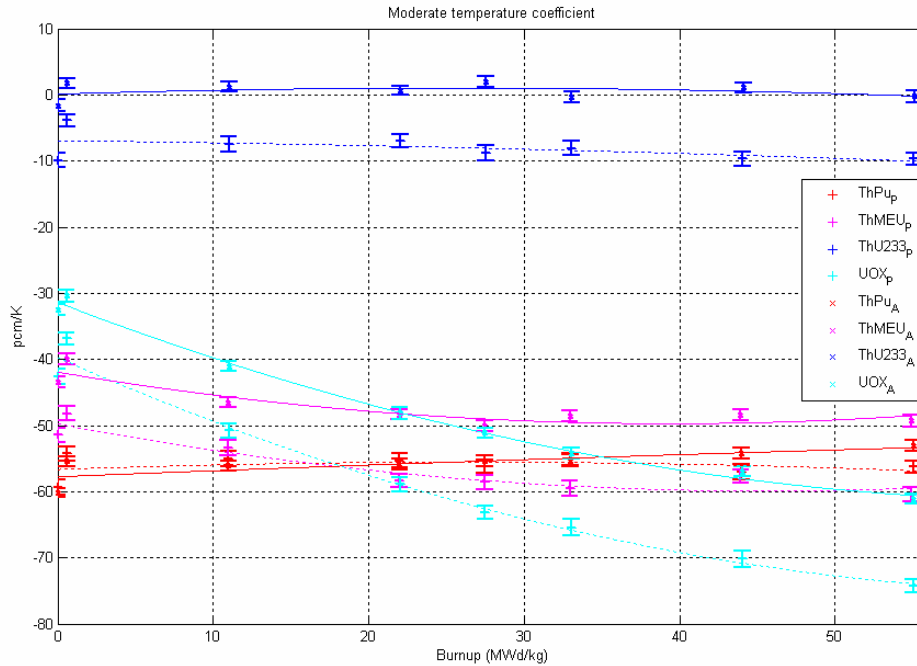


Figure 21: Moderate temperature coefficient versus burnup

The coolant temperature coefficients for $(\text{Th, Pu})\text{O}_2$, $(\text{Th, MEU})\text{O}_2$ and UOX are reasonable. The most interesting thing is that the coolant temperature coefficient of $(\text{Th, }^{233}\text{U})\text{O}_2$. It is about 10 times smaller than that of the $(\text{Th, Pu})\text{O}_2$ or UOX. It is slightly positive in assembly model. Reason can be found from the fission probabilities of ^{235}U and ^{233}U . The fission cross section of ^{235}U decreases obviously in the region of 0.1eV to 1 eV of neutron energy, but the fission cross section of ^{233}U has an obvious increase after the decrease, and it doesn't decrease greatly. The ratio which is fission cross section over the total cross section of ^{235}U shown in Figure 6 decreases about 10 times larger than for ^{233}U . Hence the fission probabilities of ^{235}U decreases 10 times larger than for ^{233}U when temperature increases, the K_∞ of UOX fuel decreases 10 times larger than for $(\text{Th, }^{233}\text{U})\text{O}_2$ fuel. MTC doesn't change linearly with burnup. It is due to the fuel composition and mass change, then the fuel to moderator ratio changes during burnup.

3.4.3. Coolant Void Worth

The coolant void worth (CVR) is the reactivity introduced when the coolant is removed. It can be calculated according to Equation(8)

$$CVR \approx k_{eff}^{void=1} - k_{eff}^{void=0} \quad (8)$$

K_{∞} is calculated separately when void is 1 and when void is 0 using MCNP. Use K_{∞} from the calculations to calculate the coolant void worth.

Figure 22 presents the coolant void worth as a function of time. The unit is pcm. One of the units of CVR is dollar (\$). It normalizes the reactivity to the delayed neutron fraction show in Equation(9). If the reactivity is 1 \$, the reactor is prompt critical which means it can be critical without delayed neutron. And the lifetime for prompt neutron is very short. So it can't be controlled. Hence, the reactivity should be less than the delayed neutron fraction.

$$1\$ = \beta \quad (9)$$

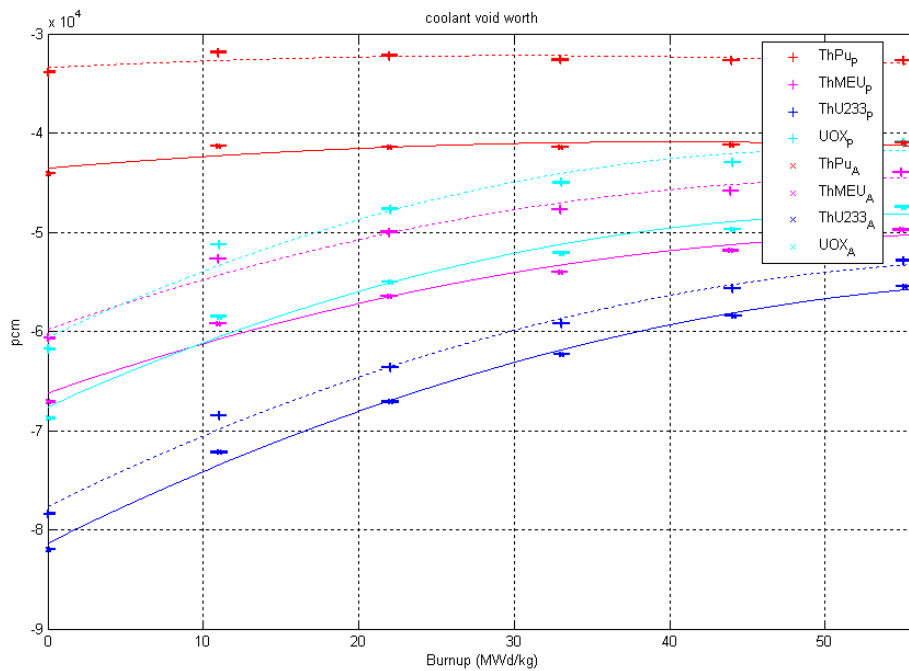


Figure 22.: Coolant void worth versus burnup(boron concentration: 500 ppm)

From Figure 22 we can find the absolute values of CVR decrease as burnup increases. The coolant is void, which means there is no moderator. The neutrons

are not slowed down and the energy of the neutron increases, the neutron spectrum becomes harder. It will make the fission cross section of some isotopes smaller and the multiplication factor decreases. During burnup, more and more fission products are produced. These kinds of isotopes will enhance the decrease of the multiplication factor. The large negative value of CVR is reasonable. Large CVR is actually a foundation for the safety of PWRs. (Th, ^{233}U) O_2 fuel has the largest CVR while (Th, Pu) O_2 has the smallest CVR and CVR for (Th, Pu) O_2 doesn't change a lot.

Figure 23 presents CVR versus boron concentration. The Red line, Magenta line and Blue line represent boron concentrations at 5 ppm, 500 ppm and 1200 ppm, respectively. The solid line and dotted line represent assembly and pin cell model.

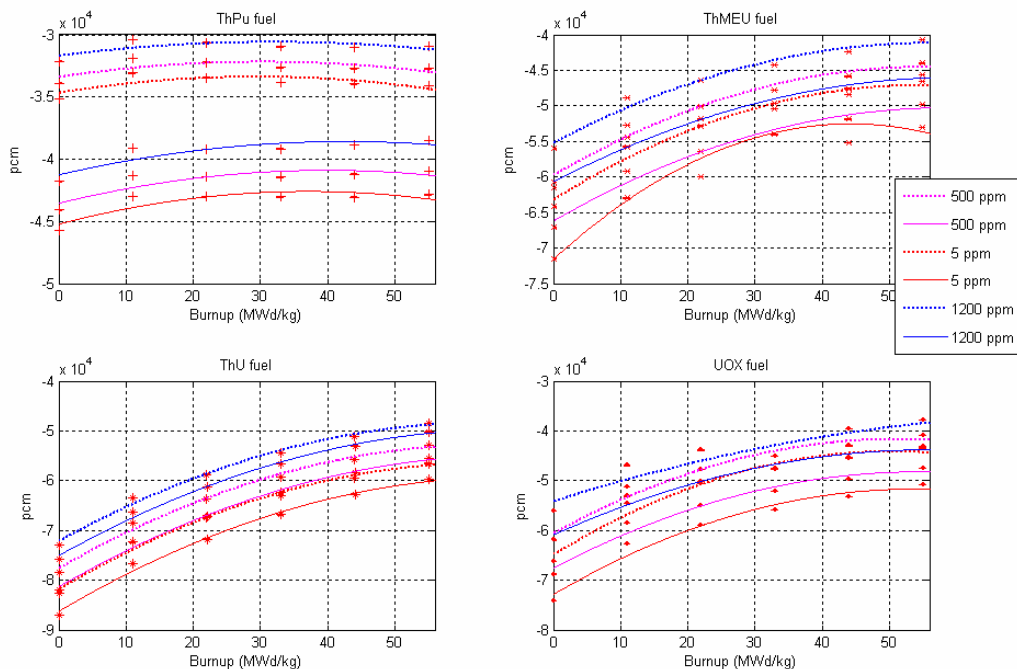


Figure 23: Coolant void worth versus boron concentration

Red line: boron concentration is 5 ppm, Magenta line: boron concentration is 500 ppm, Blue line: boron concentration is 1200 ppm, Solid line: assembly, Dotted line: pin cell, Plus sign: (Th, Pu) O_2 , Cross : (Th, MEU) O_2 , Asterisk: (Th, ^{233}U) O_2 , point: UOX.

It is clear to see, CVR is dependant on the concentration of boron and the absolute value of CVR is larger when boron concentration is small. It is because when the coolant is void, it means no moderators. When boron concentration is small, fewer neutrons are absorbed by boron and more neutrons are slowed down. So

multiplication factor during normal operation is larger, hence the CVR is more negative if boron concentration is smaller.

3.4.4. Reactivity coefficient of Boron Concentration

The boron concentration is different in different kinds of fuel models. But it is 0 ppm at end of cycle (EOC). K_{∞} at the beginning of the cycle (BOC) with certain amount of boron and saturated Xe should equate to K_{∞} at EOC with zero concentration of boron. The boron concentration is adjusted according to this point. The boron concentrations for different kind of fuel composition are show in Table 11. Reactivity coefficient of boron concentration (BCR) is calculated according to Equation(10). The results are shown in Figure 24.

Table 11: Boron concentration at BOC

Type	Pin Cell (ppm)	Assembly (ppm)
(Th, Pu)O ₂	1251	1055
(Th, MEU)O ₂	840	719
(Th, ²³³ U)O ₂	1186	1051
UOX	1327	1071

$$BCR = \frac{\rho^{C_1} - \rho^{C_2}}{C_1 - C_2} = \frac{1}{C_1 - C_2} \times \left(\frac{1}{k_{eff}^{C_2}} - \frac{1}{k_{eff}^{C_1}} \right) \quad (10)$$

Where C_1 is the values presented in Table 11 and C_2 is 100 ppm less than C_1 .

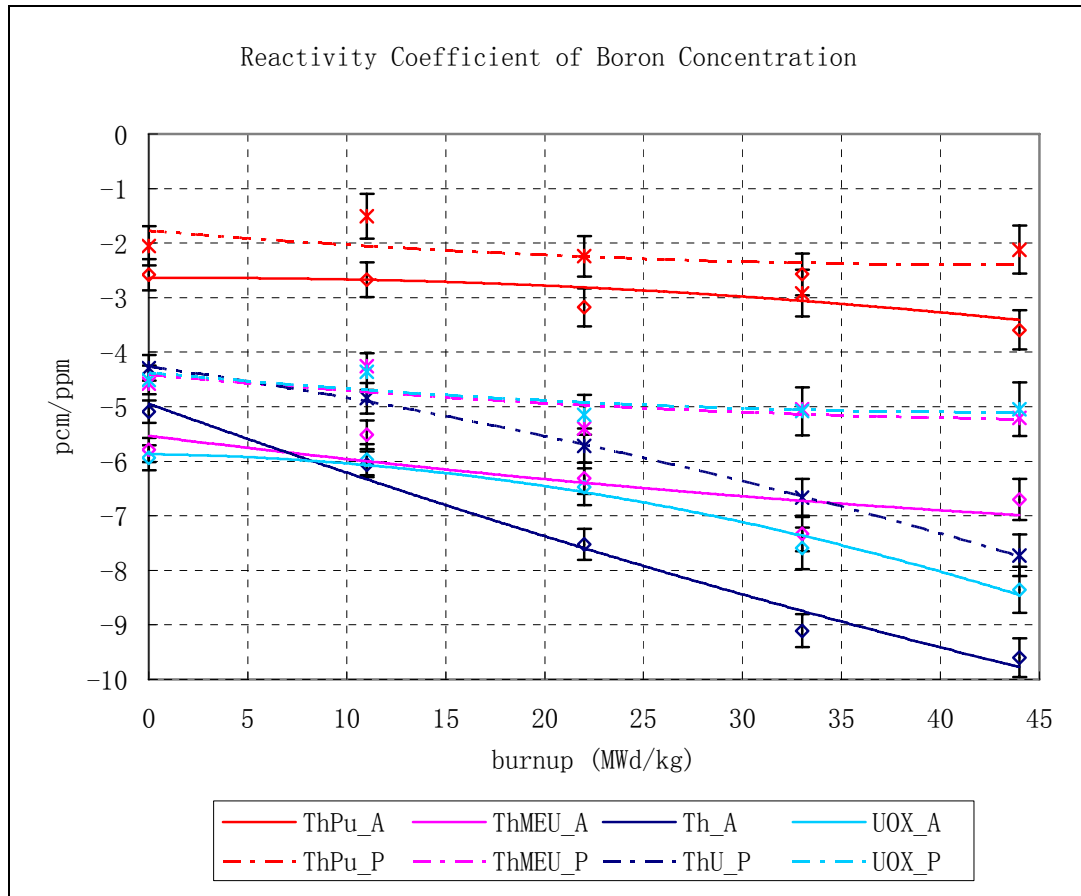


Figure 24: Reactivity coefficient of boron concentration versus boron concentration

Boron is usually used as an absorber in the reactor for reactor regulation. BCR are negative for all these fuels. (Th, Pu)O₂ has the smallest BCR. BCR for (Th, Pu)O₂ in the assembly model at burnup 33 MWd/kgH.M. is about -3 pcm/ppm. While (Th, ²³³U)O₂ fuel in assembly model has the largest value. The reason is that ²⁴⁰Pu has a much larger capture cross section than ¹⁰B has. So thermal absorption in Pu isotopes compete stronger compared to the other cases, hence the boron worth for (Th, Pu)O₂ is the weakest. BCR becomes more negative as burnup increases. A large negative value can be good for the shutdown capacity.

3.4.5. Prompt and Delayed Neutrons Parameters

Delayed neutrons are important for reactor operation. The neutrons emitted directly in fission reaction are so called prompt neutron. The neutron emitted by fission products decay are so called delayed neutron. The delayed neutrons make the fission reactor possible to be controllable. One of the important parameters is

the delayed neutron fraction. The effective delayed neutron fraction has been calculated according to Equation(11) and shown in Figure 25.

$$\beta_{eff} = \frac{k - k_p}{k} \quad (11)$$

Where, k and k_p are multiplication factor with and without delayed neutron, respectively. PHYS card and TOTNU card in MCNP are used to get these two values.

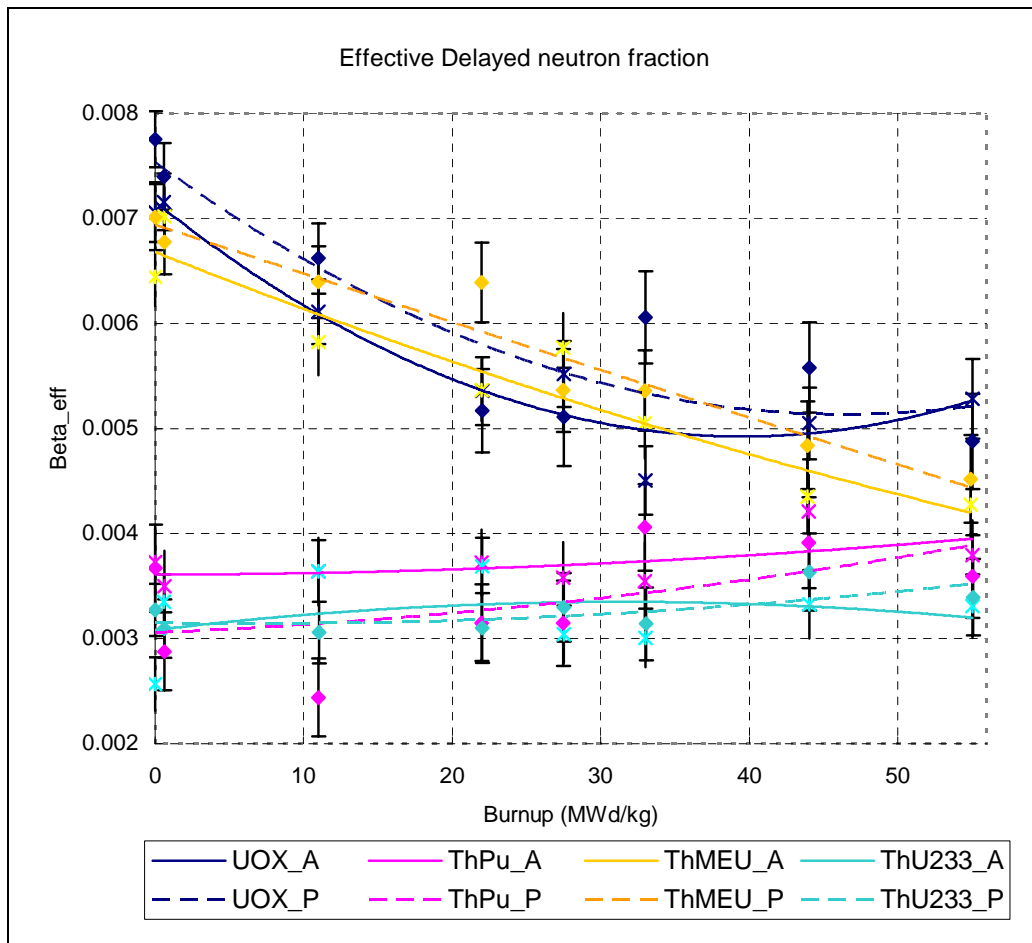


Figure 25: Effective delayed neutron fraction versus boron concentration

It is clear from the figure that uranium fuel has the largest effective delayed neutron fraction. Hence, uranium fuelled core is less easy to make prompt critical. The effective delayed neutron fractions for (Th, MEU)O₂ fuel and UOX fuel decrease with burnup, and the values for (Th, Pu)O₂ fuel and (Th, ²³³U)O₂ fuel increase slightly with burnup.

3.5. (Th, ²³³U, Pu)O₂ fuel

Based on the results presented above, an investigation on thorium fuel with mixed ²³³U and LWR spent fuel grade Pu as fissile material is carried out. The fuel composition is adjusted to satisfy K_∞ requirement and burnup requirement. And the mass of ²³³U in the fuel at discharge burnup equates to that in the fresh fuel. The density for (Th, ²³³U, Pu)O₂ fuel is about 9.17 g/cc. The weight percent is about 3.74% for Pu and 2.04% for ²³³U in pin cell model. In Assembly model, the value is about 3.77% for Pu and 2.03% for ²³³U.

Figure 26 shows the mass of ²³³U and fissile material in (Th, ²³³U, Pu)O₂ fuel model. Not only the fissile material mass in the fresh fuel is the second smallest, but also the consumption is the second smallest among all the studied fuel models. About 70% of ²⁴⁰Pu and more than 90% of ²³⁹Pu is depleted. Mass of ²³⁸Pu, ²⁴¹Pu and ²⁴²Pu doesn't change a lot. The production of Am and Cm is about 15% of consumption of ²³⁹Pu. Figure 34 and Figure 35 show the power profile. Figure 33 shows the neutron spectrum. It is clear from Figure 33 that (Th, ²³³U, Pu)O₂ creates a thermal spectrum.

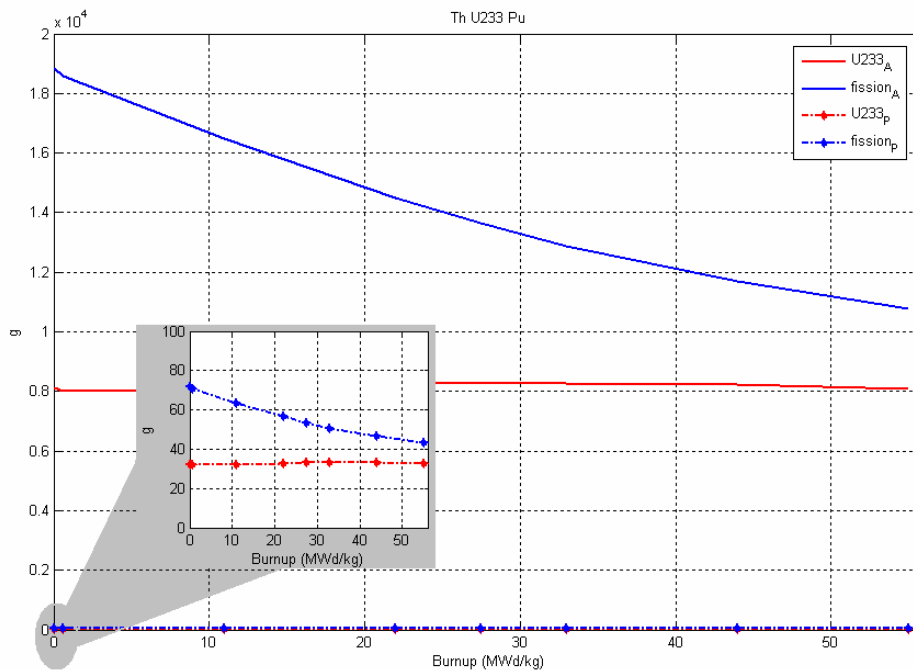


Figure 26: Evolution of masses of ²³³U and fissile material in (Th, ²³³U, Pu)O₂ fuel.

Table 12, Table 13 and Table 14 show the important neutron parameters and coefficients. All the parameters are at 33 MWd/kgH.M from assembly model. MCT of (Th, ²³³U, Pu)O₂ is larger negative than (Th, ²³³U)O₂. It is in a reasonable range. It has a better value than (Th, ²³³U)O₂ has. CVR of (Th, ²³³U, Pu)O₂ is between the values of (Th, Pu)O₂ and (Th, ²³³U)O₂. The effective delayed neutron fraction of (Th, ²³³U, Pu)O₂ is larger than the values of (Th, Pu)O₂ and (Th, ²³³U)O₂. It is better for reactor operation.

Table 12: FTR and MTC at 33 MWd/kgH.M in assembly model

Fuel	FTR (pcm/K)	MTC (pcm/K)
(Th, ²³³ U, Pu)O ₂	-3.696	-37.828
(Th, Pu)O ₂	-3.6824	-55.317
(Th, MEU)O ₂	-4.0214	-48.574
(Th, ²³³ U)O ₂	-2.9303	-0.401
UOX	-2.471	-54.179

Table 13: CVR at 33 MWd/kgH.M. in assembly model

Fuel	5 ppm	500 ppm	1200 ppm
(Th, ²³³ U, Pu)O ₂	-55515	-52859	-49418
(Th, Pu)O ₂	-43038	-41431	-39170
(Th, MEU)O ₂	-49628	-54028	-49630
(Th, ²³³ U)O ₂	-66856	-62305	-56708
UOX	-55878	-52109	-47531

Table 14: Parameters at 33 MWd/kgH.M. in assembly model

Fuel	BCR (pcm/ppm)	Beta_eff
(Th, ²³³ U, Pu)O ₂	-4.3449	0.00390
(Th, Pu)O ₂	-3.1787	0.00354
(Th, MEU)O ₂	-6.3094	0.00505
(Th, ²³³ U)O ₂	-7.5260	0.00301
UOX	-6.4700	0.00450

3.6. Shutdown Margin Check

If a reactor is shutdown, the reactor is subcritical by at least a margin. There are two kinds of shutdown situation. One is called hot shutdown. The other is called cold shutdown. In hot shutdown, the fuel temperature is reduced to the coolant temperature 300 °C, and soluble boron is also introduced into the reactor. After that, the multiplication factor should be less than 0.99, because at least 1000 pcm margin is required. The shutdown margin is defined in terms of reactivity. The units can be pcm or dollar.

Two calculations are done in hot shutdown. The maximum boron concentration allowed to introduce into the reactor is 2500 ppm. Table 16 shows K_{∞} value at different states.

Table 15: Descriptions of control rods

Parameter	Value
Absorber material	Ag-In-Cd (80 wt%, 15 wt%, 5 wt %)
Absorber diameter	0.86 cm
Absorber density	10.00 g/cc
Absorber length	366 cm
gas in the gap between absorber and cladding	air
Gas gap thickness	0.005
Cladding material	Stainless Steel
Cladding thickness	0.05 cm
Number of control rod thimble	24

In cold shutdown, the fuel temperature and the coolant temperature are 300 K. Cold shutdown is usually done after hot shutdown has been preformed for some time. The poison Xe has reached the equilibrium. Control rods are inserted into the guide thimbles. The control rod descriptions are tabled in Table 15. After the control rods are inserted, there is one month of zero power.

We can find from Table 16 that, K_{∞} for each kind of fuel either at hot shutdown or cold shutdown is less than 0.99. So, hot shutdown and cold shutdown are safe.

Table 16: K_{∞} in different conditions at burnup 22 MWd/kgH.M..

	Condition	ThPu	ThMEU	ThU	ThUPu	UOX
Normal Operation	$T_F = 900K, T_C = 600K$ $C(^{10}B) = 500ppm$	1.03307	1.04705	1.09044	1.05752	1.07589
Hot shutdown-1	$T_F = T_C = 600K$ $C(^{10}B) = 500ppm$	1.0463	1.06259	1.10111	1.06963	1.08581
Hot shutdown-2	$T_F = T_C = 600K$ $C(^{10}B) = 2500ppm$	0.98617	0.94223	0.95478	0.98383	0.95524
Cold shutdown	$T_F = T_C = 300K$ $C(^{10}B) = 2500ppm$ <i>ControlRod</i>	0.84672	0.75026	0.71009	0.94810	0.74578

4. Conclusions

Thorium fuel with four different fissile components has been studied in PWRs. Discharge burnup and power densities similar to UOX fuels are possible to achieve. Thorium fuel can satisfy the safety and operating requirements. Further more, thorium fuel has a very good proliferation resistance. The quantity and quality of the spent fuel can be improved if thorium fuel is utilized in PWRs, especially (Th, ^{233}U)O₂ fuel even doesn't create minor actinides.

Thorium fuel consumes less fissile material than uranium fuel consumes when they have the same burnup. The conversion ratio of thorium fuel is higher as well. And (Th, ^{233}U)O₂ fuel has the highest conversion ratio among the three kinds of thorium fuels here investigated. The breeding ratio of ^{233}U can be equal to one if Pu and ^{233}U are mixed correctly as fissile component.

Thorium fuel has a more negative Doppler coefficient than uranium fuel has. Hence, thorium fuel has a larger inherent, prompt feedback. (Th, ^{233}U)O₂ fuel has the most thermal neutron spectrum, the most negative coolant void worth and the largest shutdown margin, while (Th, Pu)O₂ has the hardest neutron spectrum, the smallest coolant void worth.

MTC of thorium fuel decreases more slowly than UOX fuel does when fuel is irradiated in core. (Th, ^{233}U)O₂ fuel has slight positive coolant temperature coefficient due to the fission probability of ^{233}U . However, the impact from the ratio of fuel to moderator hasn't been studied due to the time limit. Yet, coolant void worth of (Th, ^{233}U)O₂ fuel is the largest negative.

Another drawback of thorium fuel is that the effective delayed neutron fraction of thorium is smaller than uranium fuel has. Nevertheless, the characters is highly improved when mixed plutonium and ^{233}U is used as fissile components in thorium fuel. MTC of (Th, ^{233}U , Pu)O₂ is negative, and effective delayed neutron fraction is close to the value of UOX fuel.

(Th, MEU)O₂ fuel has the most negative Doppler coefficient and coolant void worth. Although, compared to UOX fuel, more uranium resources need to be concentrated in (Th, MEU)O₂ fuel, less fissile material is depleted and the quantity and quality of the spent fuel is greatly improved.

Shutdown margin are large enough for all the fuel options. It is safe in both cold shutdown and hot shutdown. As a conclusion, it is feasible to use high content thorium fuel in pressurized water reactor. The neutronic behaviors of thorium fuel

can be acceptable if proper fissile material is used. Yet, farther study is needed to find the reasons and more behaviors of thorium fuel. And study in whole core scale is necessary.

Bibliography

1. http://www.globalwarmingart.com/wiki/Image:Nuclear_Power_History_png, data from “Nuclear Power Reactors in the World”, IAEA, April 2006 Edition.
2. <http://www.iaea.org/cgi-bin/db.page.pl/pris.oprconst.htm>, “Nuclear Power Plant Information”, last update 15th January 2008.
3. Akio YAMAMOTO, “Benchmark Problem Suite for Reactor Physics Study of LWR Next Generation Fuels”, Japan, 2002.
4. Dean Wang, “Optimization of a Seed and Blanket Thorium-Uranium Fuel Cycle for Pressurized Water Reactor”, Massachusetts Institute of Technology, June 2003.
5. IAEA, “Thorium fuel cycle-Potential benefits and challenges”, Vienna, Austria, May 2005.
6. Judith F. Briesmeister, “MCNPTM-A General Monte Carlo N-Particle Transport Code”, Los Alamos National Laboratory Los Alamos, New Mexico, December 2000.
7. B. Fourest, T. Vincent. “Long-term behaviour of a thorium-based fuel”, Group de Radiochimie, Institute de Physique Nuclear, France, August 2000.
8. J.C. Gehin and R.T. Primm, “American Nuclear Society Light Water Reactor Mixed Oxide Benchmark I”, Computational Physics and Engineering Division Oak Ridge National Laboratory, July 1997.
9. IAEA, “Nuclear Power Reactors in the World”, VIENNA, 2006
10. J. Stephen Herring, Philip E. “Low cost, proliferation resistant, uranium-thorium dioxide fuels for light water reactor”, Advanced Nuclear Energy Products, Idaho National Engineering and Environment Laboratory, USA, May 2000.
11. P.K. Dey, N.K. Bansal, “Spent fuel reprocessing: A vital link in Indian nuclear power program”, Nuclear Recycle Group, Bhabha Atomic Research Centre, Trombay,,India 2005
12. Final report (1979-1988) “Thorium Utilization in PWRs”, 1988
13. Galperin, M Segev, “Radkowsky Thorium Fuel-A nonproliferative Th-based Fuel Cycle for PWRs”, Reactor Analysis Group, Ben-Gurion University of the Negev, Aerial 1999

APPENDIX

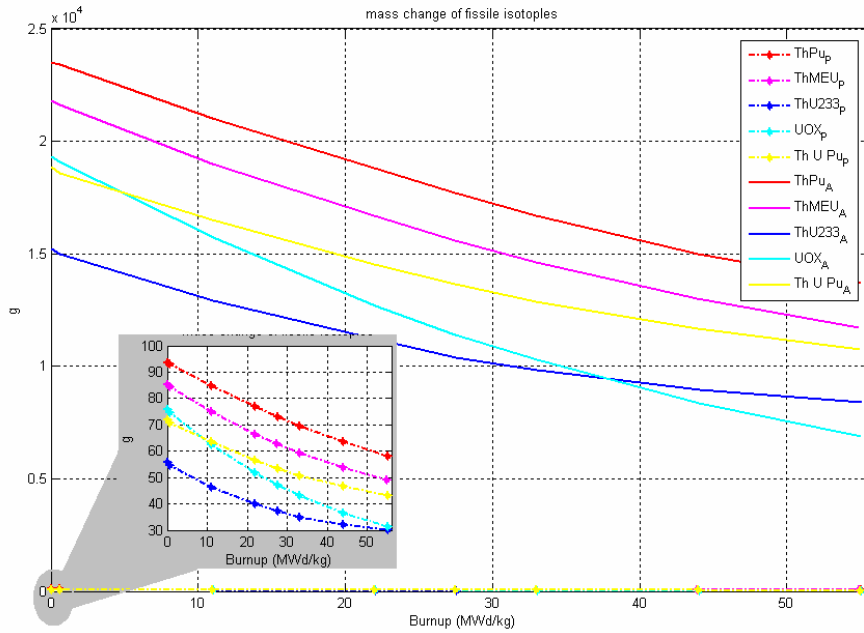


Figure 27: mass of fissile material (^{233}U ^{235}U ^{239}Pu and ^{241}Pu) for five fuel model

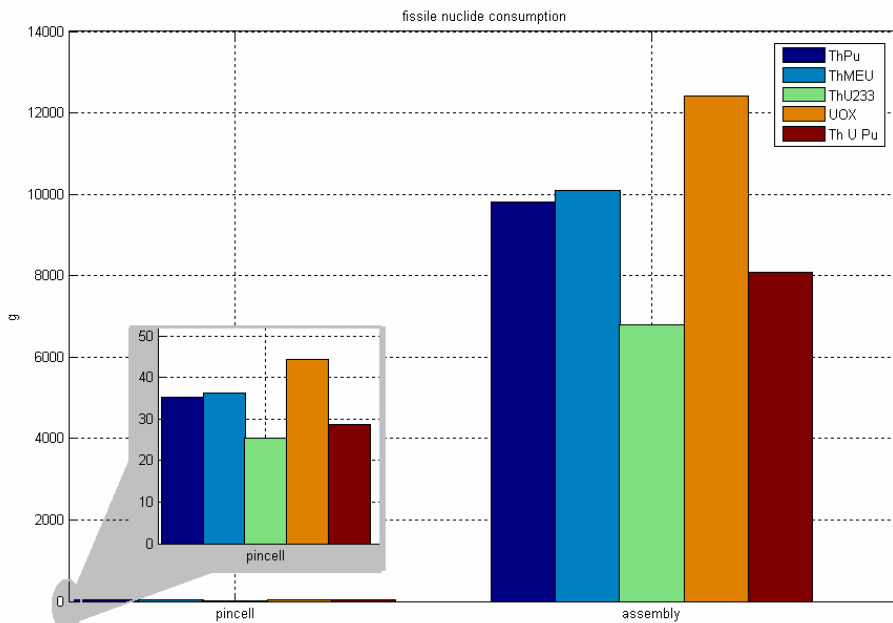


Figure 28: fissile material consumption

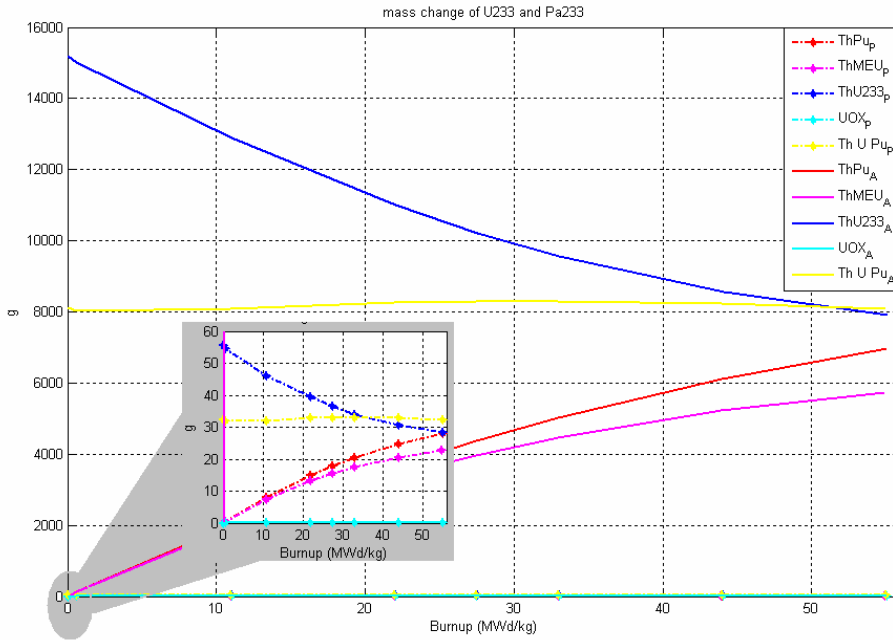


Figure 29: mass of ^{233}U and ^{233}Pa

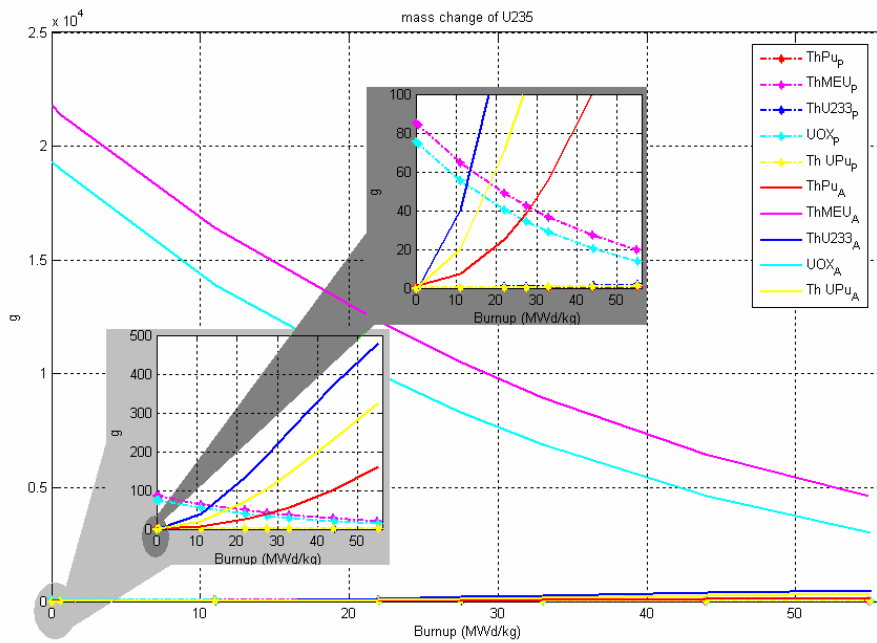


Figure 30: mass of ^{235}U

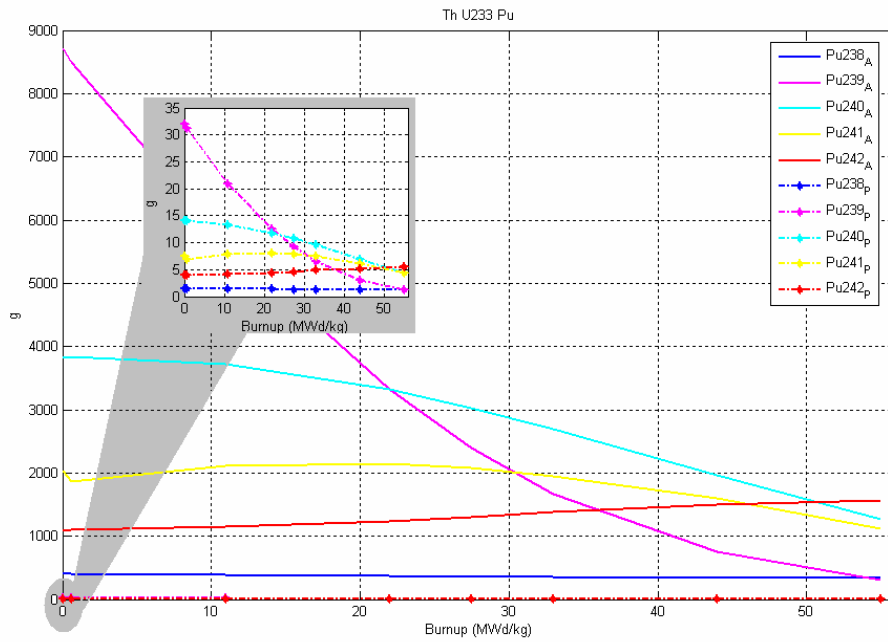


Figure 31: mass of Pu (^{238}Pu , ^{239}Pu , ^{240}Pu , ^{241}Pu and ^{242}Pu)

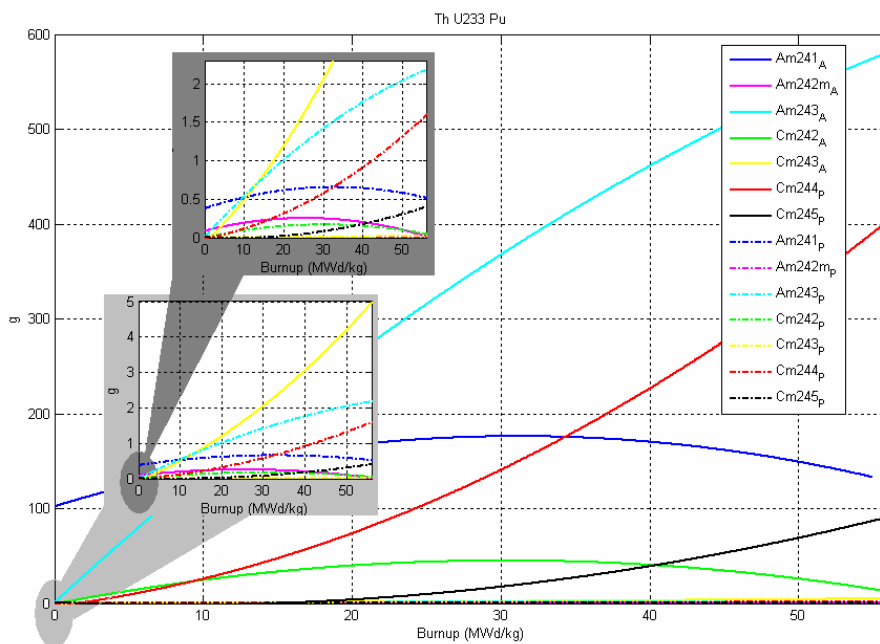


Figure 32: important minor actinides

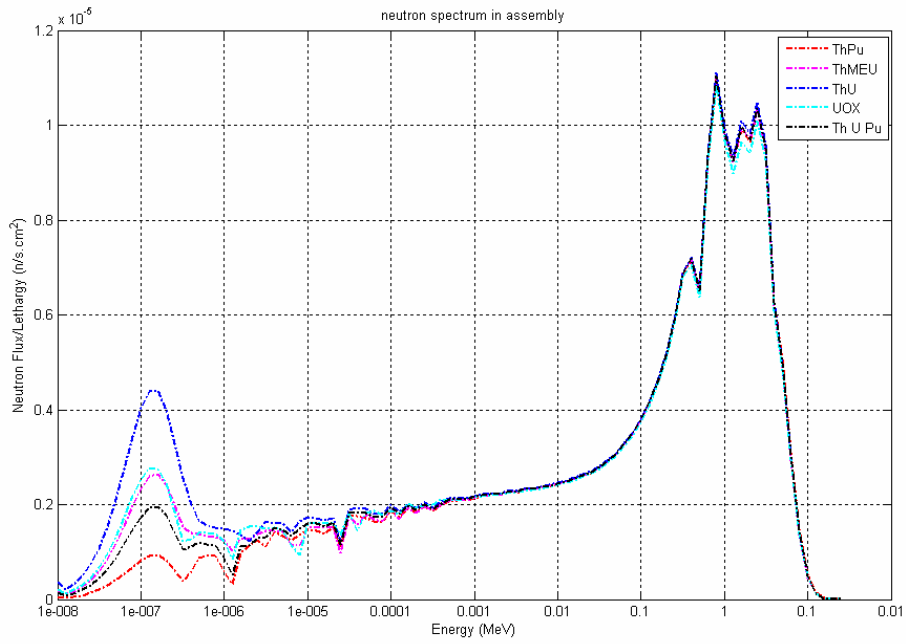


Figure 33: neutron spectrum in the fuel of assembly model

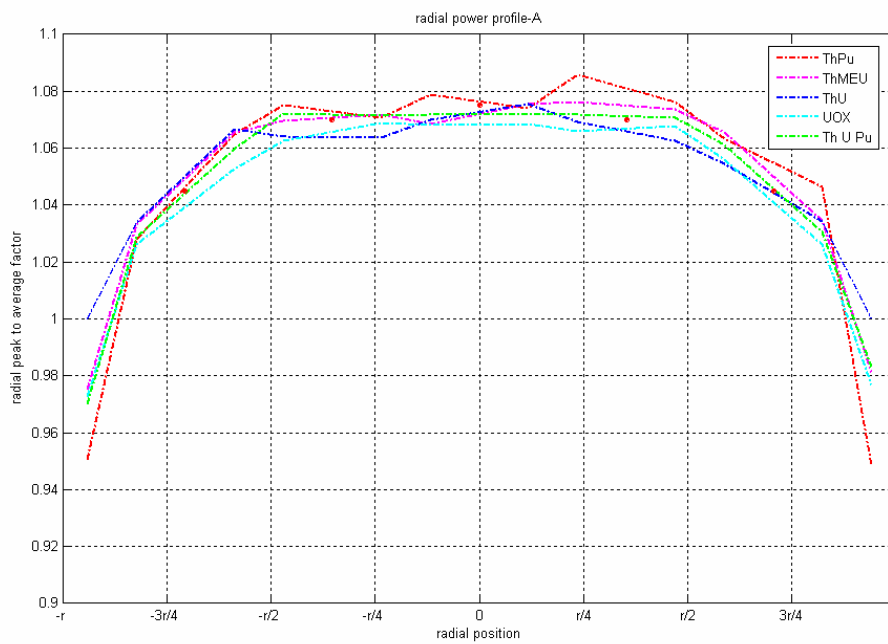


Figure 34: radial power profile of assembly model

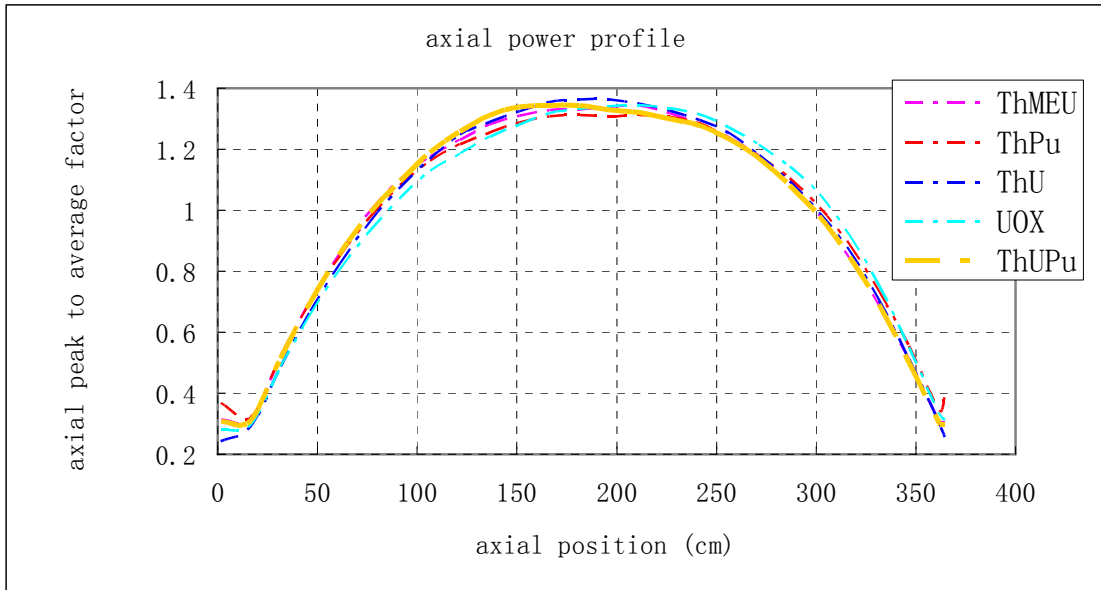


Figure 35: axial power profile of assembly model